JOURNAL OF VIROLOGY, Apr. 2004, p. 3984–3993
0022-538X/04/$08.00+0 DOI: 10.1128/JVI.78.8.3984–3993.2004

Vol. 78, No. 8

Epstein-Barr Virus Nuclear Antigen Leader Protein Induces Expression of Thymus- and Activation-Regulated Chemokine in B Cells

Mikiko Kanamori,[1,2] Shinya Watanabe,[3] Reiko Honma,[3,4] Masayuki Kuroda,[5] Shosuke Imai,[5] Kenzo Takada,[6] Naoki Yamamoto,[2] Yukihiro Nishiyama,[1] and Yasushi Kawaguchi[1,7]*

Department of Virology, Nagoya University Graduate School of Medicine, Showa-ku, Nagoya 466-8550,[1] PRESTO, Japan Science and Technology Agency, Kawaguchi, Saitama, 332-0012,[7] Department of Molecular Virology, Tokyo Medical and Dental University School of Medicine, Bunkyo-ku, Tokyo 113-8519,[2] Division of Cancer Genomics, Department of Cancer Biology, The Institute of Medical Science, The University of Tokyo, Minato-ku, Tokyo 108-8639,[3] The Japan Biological Informatics Consortium,[4] Chuo-ku, Tokyo 104-0032, Department of Molecular Microbiology and Infections Program of Bio-signaling and Infection Control, Kochi Medical School, Kochi 783-8505,[5] and Department of Tumor Virology, Institute for Genetic Medicine, Hokkaido University, Sapporo,[6] Japan

Received 28 August 2003/Accepted 11 December 2003

Epstein-Barr virus (EBV) nuclear antigen leader protein (EBNA-LP) plays a critical role in transformation of primary B lymphocytes to continuously proliferating lymphoblastoid cell lines (LCLs). To identify cellular genes in B cells whose expression is regulated by EBNA-LP, we performed microarray expression profiling on an EBV-negative human B-cell line, BJAB cells, that were transduced by a retroviral vector expressing the EBV EBNA-LP (BJAB-LP cells) and on BJAB cells that were transduced with a control vector (BJAB-vec cells). Microarray analysis led to the identification of a cellular gene encoding the CC chemokine TARC as a novel target gene that was induced by EBNA-LP. The levels of TARC mRNA expression and TARC secretion were significantly up-regulated in BJAB-LP compared with BJAB-vec cells. Induction of TARC was also observed when a subline of BJAB cells was converted by a recombinant EBV. Among the EBV-infected B-cell lines with the latency III phenotype that were tested, the LCLs especially secreted significantly high levels of TARC. The level of TARC secretion appeared to correlate with the level of full-length EBNA-LP expression. These results indicate that EBV infection induces TARC expression in B cells and that EBNA-LP is one of the viral gene products responsible for the induction.

Epstein-Barr virus (EBV) is a causative agent of infectious mononucleosis and is associated with a variety of human malignancies, including endemic Burkitt's lymphoma, nasopharyngeal carcinoma, Hodgkin's diseases, gastric carcinoma, and lymphoproliferative diseases in immunosuppressed patients (38, 51). In vitro, EBV can readily infect human B cells and cause B-cell proliferation that continues for long periods (38, 51). The lymphoblastoid cell lines (LCLs) that arise after transformation by EBV express only a limited number of the more than 80 genes (38, 51) carried on the 172-kbp EBV genome. The expressed genes include those for the EBV nuclear antigens (EBNA) EBNA-1, EBNA-2, EBNA-3A, EBNA-3B, EBNA-3C, and EBNA leader protein (EBNA-LP); the latent membrane proteins (LMP) LMP-1, LMP-2A, and LMP-2B; two small RNAs (EBV-encoded small RNAs [EBERs]); and BamA right forward transcripts (38, 51). This type of latent infection in LCLs is designated latency III (38, 51). Among the viral proteins expressed in latency III, EBNA-1, EBNA-2, EBNA-3A, EBNA-3C, EBNA-LP, and LMP-1 are critical for the process that leads to efficient differentiation of EBV-infected resting B cells into proliferating B lymphoblasts, whereas EBNA-3B, LMP-2A, LMP-2B, EBERs, and BamA right forward transcripts are not (38).

EBNA-LP, an initial gene product that is expressed together with EBNA-2 upon EBV infection of B cells (2), consists of the W1W2 multiple-repeat domain and the unique Y1Y2 C-terminal domain (Fig. 1A) (54). EBNA-LP plays a critical role in EBV-induced B-cell transformation, based on observations that recombinant EBNA-LP mutants have severely impaired transforming activity (3, 20, 41). Although the mechanism by which EBNA-LP acts in EBV-induced B-cell transformation remains unclear, several lines of evidence, listed below, suggest biological roles for the protein in the transformation process.

(i) The primary function of EBNA-LP is transcriptional coactivation with EBNA-2. EBNA-LP stimulates EBNA-2-mediated transcriptional activation of viral and cellular genes, such as those for LMP-1 and cyclin D2 (23, 46, 58). Recent studies reveal that cellular localization (44, 50, 73), phosphorylation on Ser-35 by both cellular and EBV-encoded protein kinases (including cdc2 and BGLF4) (33, 34, 74), and protein complex formation with either self (67) or cellular protein HA95 and protein kinase A (21, 22) are critical for the regulation of EBNA-LP coactivating functions.

* Corresponding author. Mailing address: Department of Virology, Nagoya University Graduate School of Medicine, 65 Tsurumai-cho, Showa-ku, Nagoya 466-8550, Japan. Phone: 81-52-744-2207. Fax: 81-52-744-2452. E-mail: ykawagu@med.nagoya-u.ac.jp.

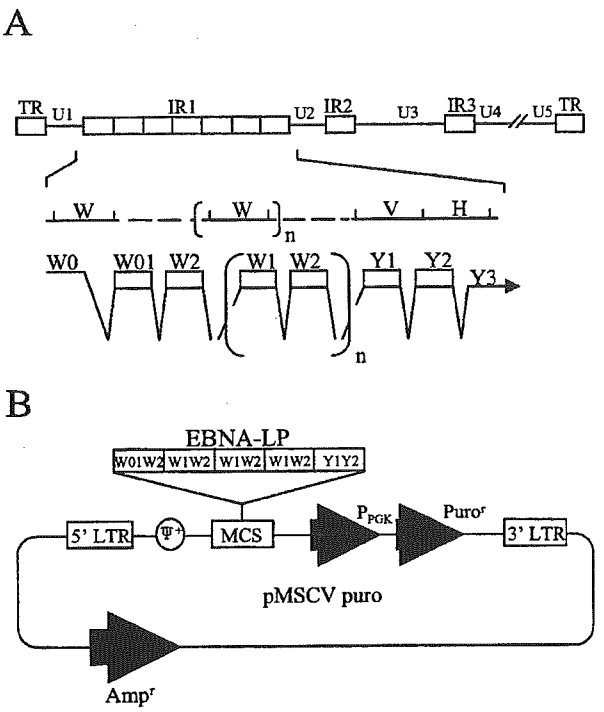

FIG. 1. (A) Schematic diagram of the sequence of the EBV genome and location of the EBNA-LP gene. The top line is a linear representation of the EBV genome. The unique sequences are represented as U1 to U5. The terminal and internal repeats flanking the unique sequences are shown as open rectangles with their designations given above the rectangles. The middle line shows an expanded section of the domain encoding the EBNA-LP gene. The exons of EBNA-LP open reading frames are derived from the BamHI W and Y fragments. The bottom line shows the structures of the EBNA-LP transcript and coding regions. (B) Schematic diagram of the retroviral vector expressing EBNA-LP used for establishment of BJAB cells stably expressing EBNA-LP (BJAB-LP cells). LTR, long terminal repeat; MCS, multiple cloning site.

(ii) EBNA-LP interacts with many cellular proteins. The cellular proteins include pRb, p53, the 70-kDa family of heat shock proteins (Hsp70), HS1-associated protein X1, α- and β-tubulins, Hsp27, HA95, protein kinase A, estrogen-related receptor 1, and bcl-2 (21, 22, 24, 36, 39, 42, 43, 64). In LCLs, EBNA-LP is localized to discrete nuclear foci called ND10, which also contain Hsp70, CBP/p300, and a distinct antigenic form of pRb (5, 31, 62, 63). Although the functional consequences of these potential interactions are unknown, the plethora of interactions implies that EBNA-LP is not only a coactivator of EBNA-2 but also a multifunctional protein that modulates various components of the cellular machinery and that the functions of EBNA-LP in EBV-induced B-cell transformation results from the sum of these interactions. Consistently, it has been recently proposed that EBNA-LP has the potential to inhibit pre-mRNA cleavage and polyadenylation (12).

The object of this report is to unveil any previously unreported, novel function(s), of EBNA-LP. The numerous interactions between EBNA-LP and various cellular components predict that additional biological activities of EBNA-LP remain unreported. Further understanding of EBNA-LP action in infected cells requires the identification of the activities. We used microarray expression profiling to identify cellular genes whose expression is regulated solely by EBNA-LP in B cells. The study results show that (i) the thymus- and activation-regulated chemokine (TARC) gene, which encodes a CC chemokine shown to selectively attract Th2-type T lymphocytes (29), is regulated; (ii) EBNA-LP up-regulates both expression of TARC mRNA and secretion of TARC protein in B cells; and (iii) EBV latency III infection induces TARC in B cells.

MATERIALS AND METHODS

Cells. Ramos is an EBV-negative Burkitt's lymphoma (BL) cell line. BJAB is an EBV-negative non-BL-type human B-cell line. P3HR1 and Raji are EBV-positive BL lines. B95-8 is a marmoset cell line carrying infectious mononucleosis-derived EBV. Peripheral blood mononuclear cells (PBMCs) from healthy volunteers were isolated by Ficoll-Paque Plus (Amersham Pharmacia Biotech) density gradient centrifugation. CD19-positive B cells were isolated from PBMCs with M-450 anti-CD19 Dynabeads (Dynal, Great Neck, N.Y.) according to the manufacture's directions. All cells were maintained in RPMI 1640 medium supplemented with 10% fetal calf serum (FCS) and antibiotics. The amphotropic retrovirus packaging cell line Bing (47) was kindly provided by W. Pear and was maintained in Dulbecco's modified Eagle's medium supplemented with 10% FCS and antibiotics.

Construction of recombinant retroviruses and retrovirus-mediated gene transfer. To construct the recombinant retroviral vector pMSCV-LP, EcoRI and PstI fragments of pGBT9-EBNA-LPR4 (36) were blunted and cloned into the HpaI site of pMSCV-puro (kindly provided by W. Pear). To produce retrovirus either with (MSCV-LP) or without (MSCV-vec) EBNA-LP, the pMSCV-LP or pMSCV plasmids were transfected into the Bing packaging cell line by calcium phosphate precipitation as described previously (48). At 48 h posttransfection, the supernatant containing amphotropic retrovirus was harvested, passed through a 0.45-μm-pore-size filter, and stored at −80°C. BJAB cells were infected with retrovirus-containing supernatant as described previously (48). At 72 h postinfection, cells were plated in flat-bottom 96-well microtiter plates in medium containing 0.4 μg/ml puromycin (Sigma). Cells were fed once a week with the same medium, and resistant cells appeared after approximately 2 weeks. Clones of resistant cells were obtained by limiting dilution on mouse primary thymocyte feeder cells.

Microarray analysis. Synthetic polynucleotides (80-mers) representing 13,440 human genes (MicroDiagnostic, Tokyo, Japan) were arrayed with a custom-made arrayer. Poly(A)$^+$ RNA was prepared from cells with TRIzol reagent (Invitrogen) and a Poly(A)Purist kit (Ambion). Two micrograms of poly(A)$^+$ RNA was labeled with Cyanine 5-dUTP or Cyanine 3-dUTP. Hybridization and subsequent washes of arrays were performed with a labeling and hybridization kit (MicroDiagnostic). Hybridization signals were measured with a GenePix 400A scanner (Axon Instruments) and then processed into primary expression ratios of Cyanine 5-labeled to Cyanine 3-labeled samples by the GenePix Pro software (Axon Instruments). A secondary ratio of expression of each gene was calculated by averaging the primary expression ratio obtained from an experiment with Cyanine 5-labeled target and Cyanine 3-labeled control samples and the reciprocal of the primary expression ratio obtained from an experiment with Cyanine 5-labeled control and Cyanine 3-labeled target samples. The secondary expression ratios calculated from the pair of experiments were converted into $\log_2$ values as the final expression ratios.

Northern blot hybridization. Total RNA from cultured cells was prepared by using ISOGEN reagent according to the instructions of the manufacturer (Nippongene). Total RNA samples were electrophoresed through 0.8% agarose gels containing 2.2 M formaldehyde and transferred to Hybond-N membranes (Amersham Pharmacia Biotech). The blots were first hybridized with the cDNA fragment probe, which encoded a part of TARC, labeled with [α-^{32}P]dCTP by using a Rediprime II labeling kit (Amersham Pharmacia Biotech) as described previously (35). After hybridization with the TARC probe, the blot was stripped by boiling in 0.1% sodium dodecyl sulfate and then rehybridized with a ^{32}P-labeled cDNA fragment encoding part of glyceraldehyde-3-phosphate dehydrogenase (G3PDH). Relative amounts of mRNA were quantified with an LAS-1000 image analyzer and the software Image Gauge (Fujifilm). The cDNAs used as probes for TARC and G3PDH were amplified by reverse transcription-PCR (RT-PCR) from RNA samples of both the BJAB cells that stably expressed EBNA-LP and the control BJAB cells. RT-PCR was performed with the Super-

TABLE 1. Primer sequences used for the amplification of TARC, BamHI W, and GAPDH genes

Amplified region (nt)	Forward primer	Reverse primer	Product size (bp)	Annealing temp (°C)[a]	No. of amplification cycles
TARC (109–370)	5′-GCACATCCACGCAGCTCGAGGGAC-3′	5′-GGGAGACAGTCAGGAGTCTGGGGT-3′	262	60	40
BamHI W (45484–45617)	5′-CAAGAACCCAGACGAGTCCGTAGAA-3′	5′-AAGAAGCATGTATACTAAGCCTCCC-3′	134	58	30
GAPDH (171–606)	5′-CATTGACCTCAACTACATGG-3′	5′-AGTGATGGCATGGACTGTGG-3′	436	60	40

[a] Denaturing was at 94°C for 60 s, annealing was at the indicated temperature for 60 s, and extension was at 72°C for 60 s.

script one-step RT-PCR system according to the instructions of the manufacturer (Invitrogen) with appropriate primer pairs and under the amplification conditions shown in Table 1. The amplified DNA fragment encoding TARC (nucleotides [nt] 109 to 370) was purified, verified by sequencing, and used as the probe. For the G3PDH probe, the amplified DNA fragment was cloned into pGEM-T Easy vector to yield pGEM-G3PDH and sequenced. The EcoRI fragment of pGEM-G3PDH encoding G3PDH (nt 171 to 606) was used as the probe. RT-PCR was performed in a 50-μl reaction solution containing 0.1 μg of RNA, using 10 pmol of each primer.

Detection of EBV genome by PCR. For detection of the EBV genome, the BamHI W region of EBV DNA was amplified by PCR from DNA isolated from EBV-infected cell cultures, and the specificity of amplification was verified by Southern blot hybridization with internal ^{32}P-labeled oligonucleotide as described previously (65, 66). For DNA extraction from cultured cells, cell pellets were subjected to one cycle of freezing and thawing, followed by addition of 50 mM NaOH. After vigorous vortexing, the solution was boiled for 10 min and neutralized with 1 M Tris-HCl (pH 8.0).

Immunoblotting. The electrophoretically separated proteins were transferred to nitrocellulose sheets and detected with antibodies as described previously (37).

Immunofluorescence. Cells were harvested, washed once with phosphate-buffered saline (PBS), and smeared onto glass slides. The cells were fixed with acetone for 10 min, blocked with PBS containing 5% goat serum for 30 min, rinsed once in PBS, reacted for either for 1 h at room temperature or overnight at 4°C with a mouse monoclonal antibody to EBNA-LP (LP-4D3), rinsed three times with PBS, reacted for 1 h with goat anti-mouse immunoglobulin G (IgG) conjugated to fluorescein isothiocyanate (Sigma), rinsed with PBS, and mounted in PBS containing 90% glycerol. The slides were examined with a Zeiss LSM 510 laser scanning microscope.

Quantification of immunoreactive TARC. A Quantikine kit (R&D Systems) for human TARC was used to quantify TARC protein secreted by cultured cells. Briefly, 10^5 cells were cultured in 48-well microplates for 3 days in RPMI medium without FCS. The supernatants were passed through 0.45-μm-pore-size filters, and TARC protein was quantified with an enzyme-linked immunosorbent assay (ELISA) system according to the instructions of the manufacturer (R&D Systems) with a microplate reader (Bio-Rad).

Virus, virus infection, and LCL assay. To establish EBV-converted cell lines, recombinant EBV (rEBV) that has the neomycin resistance gene as a selection marker inserted into BXLF1 (57) was used. rEBV was prepared from the rEBV producer cell line Akata/rEBV as described previously (25). A subline of BJAB cells, BJ-cl1R, which is more than 95% positive for CD21/CR2 (26), was converted in vitro by exposure to the rEBV, followed by selection in RPMI medium containing 0.8 mg of G418 (Sigma) per ml. To establish LCLs, EBV from culture supernatants of B95-8 cells was passed through a 0.45-μm-pore-size filter and stored at −80°C in small aliquots. PBMCs (5×10^4/well) were infected with the B95-8 supernatant in 96-well flat-bottom microtiter plates. After viral adsorption for 3 h at 37°C, the cells were cultured in fresh RPMI 1640 medium containing 8% FCS and 1 μg of cyclosporineA per ml, either with or without 500 ng of recombinant TARC (R&D Systems) per ml. Cultures without recombinant TARC were also incubated with either 1 μg of a mouse monoclonal antibody to TARC (54026.11; R&D Systems) per ml or 1 μg of a control purified IgG1 (R&D Systems) per ml. Cells were fed weekly with fresh medium for 4 weeks. The LCLs in the wells were counted and assayed for both proliferation and viability by using a Cell Counting Kit-8 (Dojindo) according to the manufacturer's instructions.

Antibodies. The mouse monoclonal antibody to EBNA-LP (LP-4D3) was generated in our laboratory with purified glutathione *S*-transferase fused to EBNA-LP (36, 67) as the antigen by using the standard procedure (17). LP-4D3 showed characteristics similar to those of JF186 (14) in immunoblotting and immunofluorescence assays (G. Matsuda, R. Furuya, C. Kamagata, and Y. Kawaguchi, unpublished observation). EBV-seropositive reference human serum (anti-EBNA1 titer, 1,280; anti-EBNA2 titer, 160) was used to detect EBNA-1 and EBNA-2. CS1-4 mouse monoclonal antibody (Dako) was used to detect LMP-1. Mouse monoclonal antibody to TARC (54026.11) was purchased from R&D Systems and β-actin antibody (AC-15) was purchased from Sigma.

RESULTS

Establishment of BJAB cell lines stably expressing EBNA-LP. To examine the effect of EBNA-LP on cellular gene expression in B cells, we used the EBV-negative human B-cell line BJAB as a starting point for construction of a cell line that

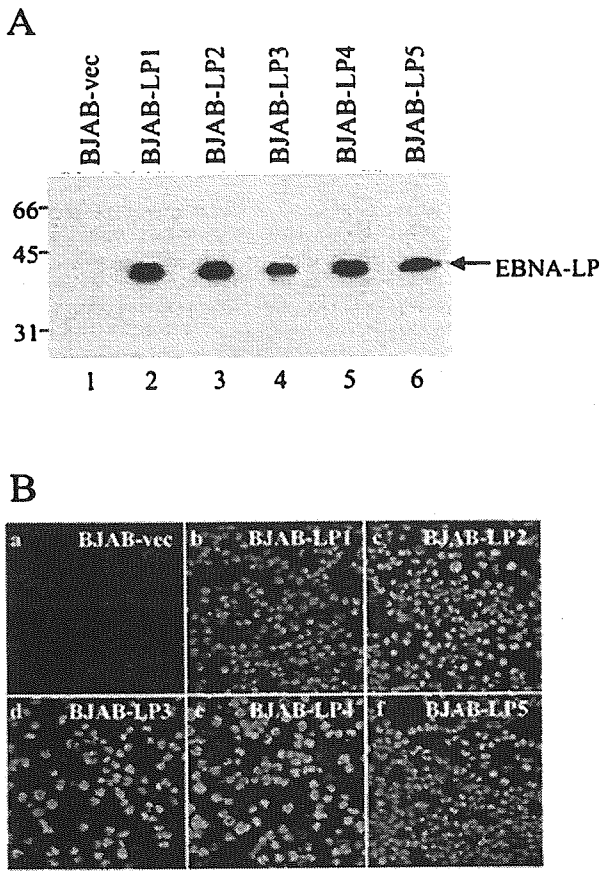

FIG. 2. (A) Immunoblot of electrophoretically separated cell lysates from BJAB-vec (lane 1) and BJAB-LP1 to BJAB-LP5 (lanes 2 to 5) cells. The cells were harvested and immunoblotted with the mouse monoclonal antibody to EBNA-LP (LP-4D3). Molecular weights (in thousands) are shown on the left. (B) Digital images of BJAB-vec (a) and BJAB-LP1 to BJAB-LP5 (b to f) from immunofluorescence assays. The cells were smeared on glass slides, fixed, and reacted with the EBNA-LP antibody (LP-4D3) and anti-mouse IgG conjugated to fluorescein isothiocyanate.

stably expressed EBNA-LP (BJAB-LP). A recombinant retrovirus encoding EBNA-LP (MSCV-LP) was generated by transfection of a recombinant retroviral vector containing EBNA-LP cDNA (pMSCV-LP) into the Bing packaging cell line. The BJAB cells were infected with MSCV-LP, and infected cells were selected with puromycin. The puromycin-resistant cells were cloned by limiting dilution, and five clones (BJAB-LP1 to BJAB-LP5) were selected. Puromycin-resistant BJAB cells infected with only MSCV-vec (BJAB-vec) were also generated as controls. Only cell clones derived from MSCV-LP infection expressed EBNA-LP, as determined by both immunoblotting (Fig. 2A) and immunofluorescence assays (Fig. 2B).

Microarray analysis of BJAB cells stably expressing EBNA-LP. RNA was extracted from a mixture of the five independent clones of BJAB-LP cells and compared with RNA from BJAB-vec cells by using the microarray with synthetic polynucleotides representing 13,440 human genes. Fourteen genes were identified by the criterion of a more-than-twofold change in expression ratio (Fig. 3). The gene for the CC chemokine TARC was selected for further characterization, since the change in expression of TARC was the highest among the 14 genes and it

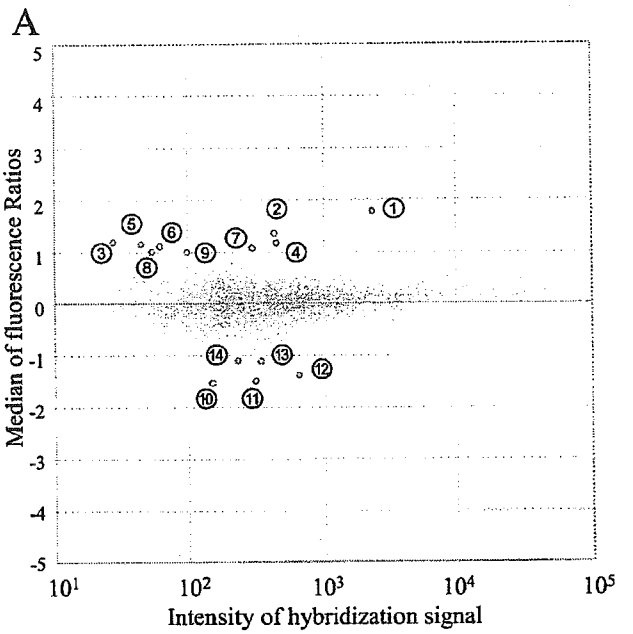

B

	Gene	GenBank Accession No.	Fold Increase
	Induced genes		
①	Thymus and activation regulated chemokine (TARC), mRNA	NM002987	3.43
②	hypothetical protein FLJ20647 (FLJ20647), mRNA.	NM017918	2.60
③	secreted phosphoprotein 1 (osteopontin, bone sialoprotein I, early T-lymphocyte activation 1) (SPP1), mRNA.	NM000582	2.30
④	hypothetical protein FLJ21079 (FLJ21079), mRNA.	NM024576	2.27
⑤	absent in melanoma 2 (AIM2), mRNA.	NM004833	2.23
⑥	KIAA1084 protein (KIAA1084), mRNA.	NM014910	2.20
⑦	anaphase-promoting complex 10 (APC10), mRNA.	NM014885	2.11
⑧	zinc finger protein 157 (HZF22) (ZNF157), mRNA.	NM003446	2.03
⑨	phosphorylase kinase, beta (PHKB), mRNA.	NM000293	2.01
	Suppressed genes		
⑩	putative prostate cancer tumor suppressor (N33), mRNA.	NM006765	-2.89
⑪	interleukin 10 (IL10), mRNA.	NM000572	-2.81
⑫	aldehyde dehydrogenase 1, soluble (ALDH1), mRNA.	NM000689	-2.62
⑬	Janus kinase 3 (a protein tyrosine kinase, leukocyte) (JAK3), mRNA.	NM000215	-2.15
⑭	annexin A1 (ANXA1), mRNA.	NM000700	-2.14

FIG. 3. Effect of EBNA-LP on cellular gene expression. (A) Microarray analysis. Poly(A)$^+$ RNA was isolated from BJAB-LP or BJAB-vec cells, labeled with different fluorescent dyes, and hybridized with a microarray that had synthetic polynucleotides representing 13,440 human genes. Hybridization signals were then analyzed. One dot corresponds to one cellular gene. The fluorescence ratio was represented as $\log_2$ (BJAB-LP/BJAB-vec). Fourteen genes whose fluorescence ratios were greater than 1 are numbered. (B) List of cellular genes whose expression was changed twofold or more by EBNA-LP protein.

has been reported that chemokines play various roles in herpesvirus infections (1).

EBNA-LP increases the level of TARC in B cells. To validate the results from microarrays showing that TARC is induced by expression of EBNA-LP in B cells, we first compared the steady-state levels of TARC mRNA in BJAB-LP cells expressing EBNA-LP and control BJAB-vec cells by Northern blot analysis. The steady-state levels of TARC mRNA in both BJAB-LP1 and BJAB-LP2 cells were increased by more than 10-fold compared with TARC mRNA levels in BJAB-vec cells (Fig. 4A and B). Similar results were obtained with BJAB-LP3 to -LP5 (data not shown). In contrast, the G3PDH mRNA levels in all of the cell lines remained unchanged (Fig. 4A and data not shown). The levels of TARC protein in the supernatants of BJAB-LP1 cells were 6.6-fold higher than those in supernatants from BJAB-vec cells (Fig. 4C). These results show that EBNA-LP up-regulates the level of TARC expression in B cells.

EBV latency III infection also increases the level of TARC in B cells. We tested whether TARC was induced not only by constructed EBNA-LP overexpression but also by EBNA-LP expression in EBV infection in B cells. The BJ-cl1R subclone of BJAB cells was infected with rEBV carrying a neomycin resistance gene to allow selection. The neomycin-resistant BJ-cl1R/rEBV cells represented type III EBV infection, since the presence of the EBV genome was detected by PCR and Southern blot analysis (Fig. 5A) and expression of EBNA-1, EBNA-2, EBNA-LP, and LMP1 in BJ-cl1R/rEBV cells was detected by immunoblotting (Fig. 5B). The expression of TARC in BJ-cl1R/rEBV cells was compared with expression in the parental BJ-cl1R cells by Northern blot analysis, and the relative amounts of TARC mRNA were normalized to those of G3PDH mRNA. The steady-state level of TARC mRNA in BJ-cl1R/rEBV cells was greater than twofold higher than that in BJ-cl1R cells (Fig. 5C and D). The TARC secretion in the supernatant of BJ-cl1R/rEBV cells, detected by ELISA, was consistently increased compared with that in the supernatant of BJ-cl1R cells (Fig. 5E). These results indicate that EBV infection induces TARC expression in B cells.

LCLs secrete high levels of TARC. To pursue the correlation between TARC induction and EBNA-LP expression in B cells with the latency III phenotype, we examined expression of TARC in primary B cells, Ramos cells, P3HR1 cells, Raji cells, B95-8 cells, and LCLs. EBV infection was confirmed by the detection of the EBV genome (Fig. 6A) and expression of EBNA-LP (Fig. 6D). As reported previously (14), EBNA-LP was detected in immunoblots as multiple protein species, depending upon the cell line, since EBNA-LP has the W1W2 multirepeat domain (Fig. 6D). The expression level of EBNA-LP in each cell line was variable. LCLs and P3HR1 cells expressed relatively abundant EBNA-LP, while Raji and B95-8 cells showed much lower levels of expression (Fig. 6D). Northern blot analysis revealed that the mRNA levels of TARC in the EBV-infected cells were variable (Fig. 6B). TARC expression was barely detectable in P3HR1, Raji, B95-8, and control Ramos and primary B cells (Fig. 6B). In contrast, the mRNA levels of TARC in LCLs were significantly higher than those in the other cell lines. Consistently, LCLs secreted a significantly higher level of TARC protein than primary B cells and the Ramos, P3HR1, Raji, and B95-8 cell

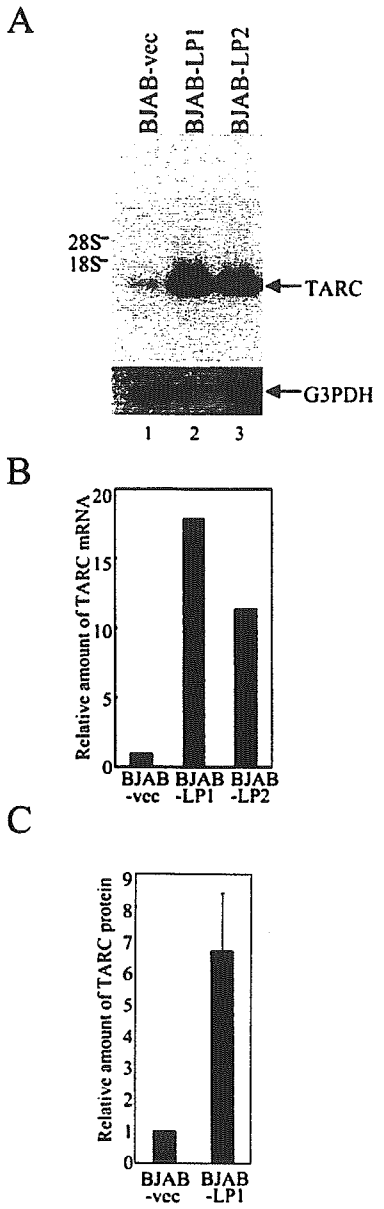

FIG. 4. Effect of EBNA-LP on TARC expression. (A) Steady-state levels of TARC or G3PDH mRNA in BJAB-LP and BJAB-vec cells. Total RNAs isolated from BJAB-vec (lane 1), BJAB-LP1 (lane 2), or BJAB-LP2 (lane 3) cells were fractionated by electrophoresis on an agarose-formaldehyde gel and analyzed by Northern blot analysis with ^{32}P-labeled probe DNAs. Locations of the 28S and 18S rRNAs are indicated on the left. (B) Quantification of relative amounts of TARC mRNA in the indicated cell lines. The relative amounts of TARC mRNA were normalized to those of G3PDH, and the results are shown as values relative to that for BJAB-vec. (C) Quantification of relative amounts of TARC protein secreted in supernatants of the indicated cell lines. The amounts of TARC protein in the supernatants were measured by ELISA, and the results are shown as a value relative to that for BJAB-vec. The results represent averages from five independent experiments, and the standard deviation is presented.

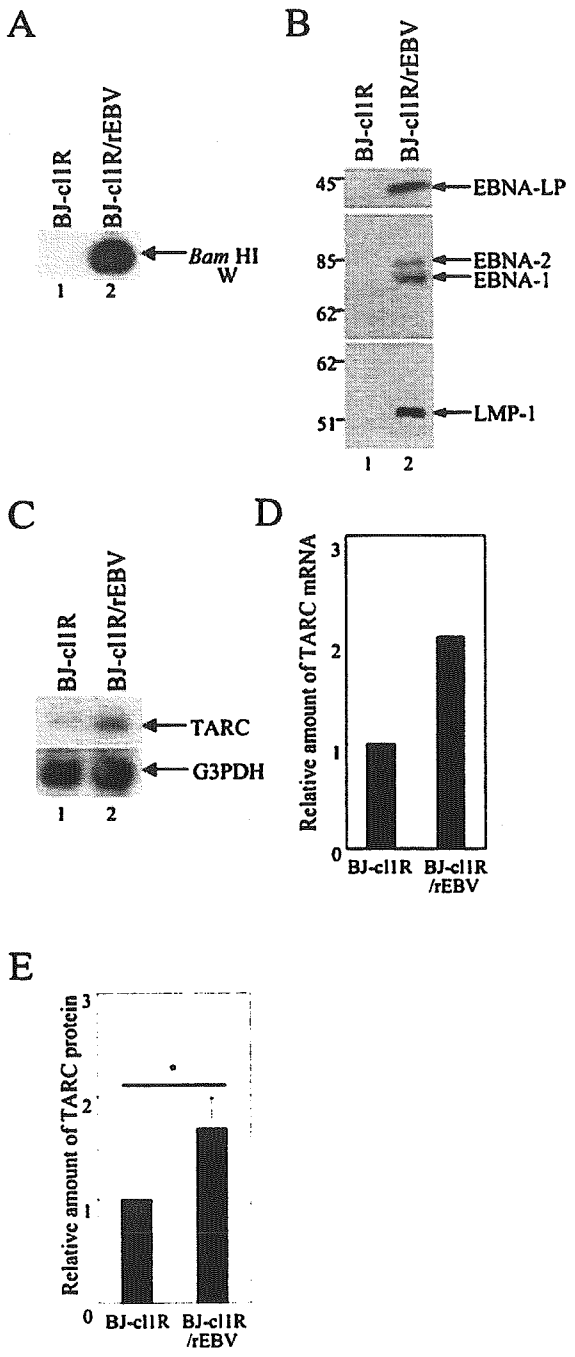

FIG. 5. EBV infection induces TARC expression in B cells. (A) The EBV genome in BJ-cl1R (lane 1) or BJ-cl1R/rEBV (lane 2) cells was detected by PCR followed by Southern blot analysis. (B) Expression of EBNA-1, EBNA-2, EBNA-LP, and LMP-1 in BJ-cl1R (lane 1) and BJ-cl1R/rEBV (lane 2) cells was examined by immunoblotting. Molecular weights (in thousands) are shown on the left. (C) Steady-state levels of TARC or G3PDH mRNA in BJ-cl1R (lane 1) and BJ-cl1R/rEBV (lane 2) cells were analyzed by Northern blot analysis. Experiments were done exactly as described in the legend for Fig. 4A. (D) Quantification of the relative amounts of TARC mRNA in the indicated cell lines. The relative amounts of TARC mRNA were normalized to those of G3PDH, and the results are shown as a value relative to that with BJ-cl1R cells. (E) Quantification of the relative amounts of TARC protein secreted in the supernatants of the indicated cell lines. Experiments were done exactly as described in the legend for Fig. 4C. The results are shown as a relative value to that with BJ-cl1R. The results represent averages from four independent experiments, and the standard deviations are presented. *, $P < 0.05$.

lines (Fig. 6C). TARC secretion appeared to correlate with expression of EBNA-LP (Fig. 6C and D). P3HR1 cells were the exception, since levels of TARC secretion were barely detectable even though the cells expressed relatively abundant EBNA-LP. However, the genome of EBV in P3HR1 has a deletion in the region encoding EBNA-2, as well as a deletion of the Y1Y2 domain of EBNA-LP. Therefore, the cells express defective EBNA-LP that contains only W repeat domains (30).

Lack of effect of TARC on EBV-induced B-cell transformation. The effect of TARC on EBV-induced B-cell transformation was examined. Normal human PBMCs were infected with EBV, either with or without TARC. The cultures were also incubated with either TARC-neutralizing antibody (54025.11) or a control purified IgG1. The efficiency with which LCLs were established was not influenced by the presence of either TARC or TARC antibody (data not shown). These results indicate that TARC is not directly involved in EBV-induced B-cell transformation.

DISCUSSION

The key finding of our study is that the EBNA-LP is able to stimulate expression of a T-cell chemoattractant, TARC, in the absence of other EBV proteins. To our knowledge, this is the first example of a cellular gene whose expression is stimulated by EBNA-LP alone. The important aspects of this study are as follows.

(i) Microarray analysis identified TARC as a novel target of EBNA-LP. In microarray analysis, we identified several candidate genes that are regulated in response of EBNA-LP expression in B cells. We focused on the TARC gene, since the change in expression of TARC that was mediated by EBNA-LP was the highest among the candidate genes. The up-regulation of TARC mRNA, mediated by EBNA-LP, was confirmed by Northern blot analysis, and the up-regulation of TARC protein levels was verified by ELISA. These results reinforced the evidence obtained by microarray analysis that TARC expression in B cells is stimulated by EBNA-LP.

(ii) EBV latency III infection induces TARC expression in B cells. EBV-negative BJAB cells that were converted to EBV positivity by rEBV infection expressed more TARC mRNA and secreted higher levels of TARC protein than parental cells. These data provide additional support for the conclusion that EBV infection stimulates TARC expression in B cells. These results also eliminate the possibility that induction of TARC in B cells by EBNA-LP was a consequence of genetically engineered overexpression of the protein by a retrovirus vector. Furthermore, we found a potential correlation between TARC secretion and EBNA-LP expression in EBV-infected cell lines with a latency III phenotype. LCLs expressed abundant EBNA-LP and secreted a significantly high level of TARC protein, while Raji and B95-8 cells exhibited low levels of expression of both EBNA-LP and TARC. P3HR1 was exceptional in that it showed high levels of EBNA-LP expression

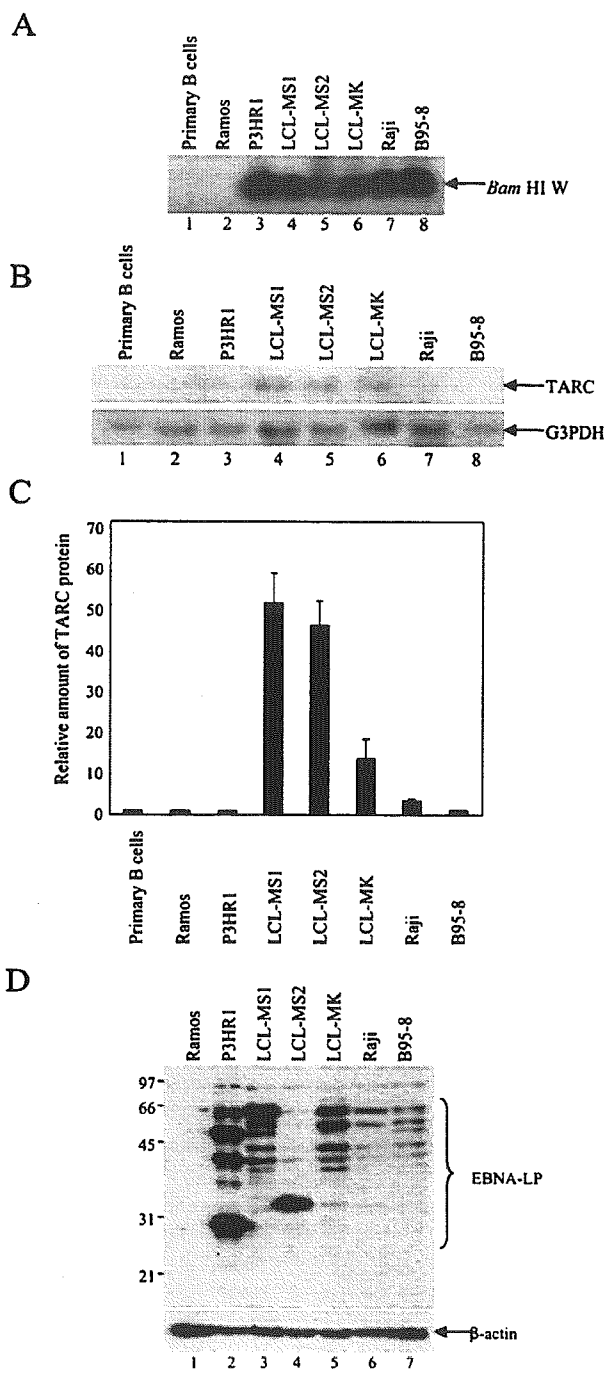

FIG. 6. TARC expression in EBV-negative and -positive B-cell lines. (A) EBV genomes in the indicated cells and cell lines were analyzed by PCR followed by Southern blot analysis. (B) Steady-state levels of TARC or G3PDH mRNA in the indicated cells and cell lines were examined by Northern blot analysis. (C) Quantification of the relative amounts of TARC protein secreted in the supernatants of the indicated cells and cell lines. Experiments were done exactly as described in the legend for Fig. 4C. The results are shown as values relative to those for Ramos cells. The results represent averages from three independent experiments, and standard deviations are presented. (D) Expression of EBNA-LP or β-actin protein in the indicated cell lines was analyzed by use of immunoblots probed with the EBNA-LP antibody (LP-4D3). Molecular weights (in thousands) are shown on the left.

but no TARC secretion. This is probably because P3HR1 has a deletion in the carboxyl-terminal domain of EBNA-LP as well as the whole region encoding EBNA-2. These results suggest that functional EBNA-LP expression is required for TARC induction. As described in the introduction, EBNA-LP is a coactivator of EBNA-2 (23, 46, 58). We also performed similar microarray analysis with BJAB cells stably expressing EBNA-2. The results were that EBNA-2 was not able to induce TARC in B cells, suggesting that EBNA-2 may not be involved in the induction of TARC in EBV-infected B cells (data not shown).

Our data support our hypothesis that EBV infection induces TARC expression in B cells and that the EBNA-LP is the viral gene product responsible for the induction. The relevant issues are as follows.

(i) Chemokines, a family of low-molecular-weight proteins, play an essential role in providing directional cues for the trafficking of leukocytes to sites of inflammation (72). A growing body of evidence suggests that their function is not restricted to chemotaxis, since they have been implicated in cell proliferation (7, 19), cell adhesion (40, 68), angiogenesis (61), and apoptosis (69). Conserved cysteine residues that are appropriately spaced are the hallmark of the two major subfamilies of chemokines, designated CXC and CC (9). TARC is the first CC chemokine shown to selectively attract T lymphocytes (29). TARC is a functional ligand for CC chemokine receptor 4, which is selectively expressed on Th2 cells (27) and induces chemotaxis of Th2-type $CD4^+$ T lymphocytes in vitro (28). Consistent with the in vitro data, it has been reported that TARC is associated with Th2-type diseases, such as atopic dermatitis and bronchial asthma (18, 32, 55, 56, 71). TARC, therefore, plays a key role in regulating the trafficking and effector functions of Th2 cells. These features of TARC render it an ideal target for a viral protein such as EBNA-LP, since it is well known that some viruses, including EBV, have evolved mechanisms to evade detection and ultimately deregulate the host immune response.

(ii) A role for chemokines in virally encoded functions is shared by herpesviruses. Both beta- and gammaherpesviruses have the ability to modify the cellular chemokine environment, by encoding either chemokines, chemokine homologues, or chemokine receptors (1). The physiological roles of the virally encoded, chemokine-related activities are unknown. However, accumulating evidence suggests that they play roles in viral dissemination (15, 49, 53, 75), viral pathogenesis (6), and the immune response (10, 13, 59, 60). Since some herpesviruses encode homologues in their genome, whereas others encode viral proteins that modulate the level of chemokines, it is conceivable that herpesviruses employ different mechanisms for affecting chemokine activity.

(iii) The biological significance of the TARC induction mediated by EBNA-LP is unclear. One hypothesis is that TARC induction is beneficial to EBV-induced B-cell transformation and survival of infected cells. TARC is a chemoattractant for Th2-type $CD4^+$ T cells (28), which express both CD40 ligand and Th2 cytokines such as interleukin-4 that induce B-cell activation (4). Th2-type $CD4^+$ T cells may be attracted to EBV-infected B cells by EBNA-LP-induced TARC and stimulate the infected B cells by the effects of CD40 ligand and interleukin-4. Earlier reports that the development of EBV-

driven human B-cell lymphoproliferative disorders and tumors in SCID/hu mice is dependent on the presence of T cells, especially $CD4^+$ T cells (8, 70), support this possibility. In addition, EBV-specific $CD4^+$ T cells mediate activation of resting B cells and induction of expression of viral BZLF1, a viral lytic cycle transactivator, in latently infected B cells via the CD40 ligand- and CD40-dependent pathway (16). Furthermore, it is well established that Th2 cytokines down-regulate the Th1 immune response (11, 52). As suggested from the model of Kaposi's sarcoma-related herpesvirus-encoded chemokines (10, 13, 59, 60), TARC induced by EBNA-LP may drive the immune response from a Th1- towards a Th2-type by recruitment of Th2-type T cells. This immunomodulatory action may be involved in immune evasion of EBV-infected B cells.

An alternative hypothesis is that the TARC induced by EBNA-LP functions as an autocrine factor for activation of chemokine receptors, which is known to modulate pathways typical of those attributed to growth factor-mediated cell activation and induction of cell proliferation (72). However, this possibility is made less likely by the previous report that peripheral blood resting B cells, EBV-immortalized B cells, and the EBV-positive BL lines (Akata, Daudi, Raji, Jijoye, and AG876) do not express CC chemokine receptor 4 (45). Consistently, the presence of excess amounts of TARC or the neutralizing antibody to TARC had no effect on EBV-induced B-cell transformation (data not shown). Furthermore, the Janus-associated kinase-STAT, mitogen-activated protein kinase pathway, and focal adhesion kinase activation, all of which can be engaged following chemokine receptor activation (72), remained unchanged when EBNA-LP was overexpressed in B cells (data not shown).

In conclusion, the EBV regulatory protein EBNA-LP is able to induce TARC expression in B cells. The biological significance of the TARC induction mediated by EBNA-LP is unknown. Further experimentation is clearly important to determine the full range of biological activities of TARC, as well as to investigate a possible role in immune evasion during EBV infection.

ACKNOWLEDGMENTS

We thank E. Kieff for EBNA-LP cDNA and E. Pear for pMSCV-puro and Bing. We thank E. Iwata, T. Tsuruguchi, and H. Noma for technical assistance. We also thank all of the members of our laboratory for helpful discussions.

This study was supported in part by Grants-in-Aid for Scientific Research (to Y.K. and Y.N.) and Grants-in-Aid for Scientific Research in Priority Areas (to Y.K. and Y.N.) from the Ministry of Education, Culture, Science, Sports and Technology (MEXT) of Japan and the Japan Society for the Promotion of Science (JSPS).

REFERENCES

1. **Alcami, A.** 2003. Viral mimicry of cytokines, chemokines and their receptors. Nat. Rev. Immunol. **3**:36–50.
2. **Alfieri, C., M. Birkenbach, and E. Kieff.** 1991. Early events in Epstein-Barr virus infection of human B lymphocytes. Virology **181**:595–608.
3. **Allan, G. J., G. J. Inman, B. D. Parker, D. T. Rowe, and P. J. Farrell.** 1992. Cell growth effects of Epstein-Barr virus leader protein. J. Gen. Virol. **73**: 1547–1551.
4. **Banchereau, J., P. de Paoli, A. Valle, E. Garcia, and F. Rousset.** 1991. Long-term human B cell lines dependent on interleukin-4 and antibody to CD40. Science **251**:70–72.
5. **Bandobashi, K., A. Maeda, N. Teramoto, N. Nagy, L. Szekely, H. Taguchi, I. Miyoshi, G. Klein, and E. Klein.** 2001. Intranuclear localization of the transcription coadaptor CBP/p300 and the transcription factor RBP-Jk in relation to EBNA-2 and -5 in B lymphocytes. Virology **288**:275–282.
6. **Boshoff, C., Y. Endo, P. D. Collins, Y. Takeuchi, J. D. Reeves, V. L. Schweickart, M. A. Siani, T. Sasaki, T. J. Williams, P. W. Gray, P. S. Moore, Y. Chang, and R. A. Weiss.** 1997. Angiogenic and HIV-inhibitory functions of KSHV-encoded chemokines. Science **278**:290–294.
7. **Broxmeyer, H. E., B. Sherry, L. Lu, S. Cooper, C. Carow, S. D. Wolpe, and A. Cerami.** 1989. Myelopoietic enhancing effects of murine macrophage inflammatory proteins 1 and 2 on colony formation in vitro by murine and human bone marrow granulocyte/macrophage progenitor cells. J. Exp. Med. **170**:1583–1594.
8. **Coles, R. E., T. J. Boyle, J. M. DiMaio, K. R. Berend, D. F. Via, and H. K. Lyerly.** 1994. T cells or active Epstein-Barr virus infection in the development of lymphoproliferative disease in human B cell-injected severe combined immunodeficient mice. Ann. Surg. Oncol. **1**:405–410.
9. **Curnock, A. P., M. K. Logan, and S. G. Ward.** 2002. Chemokine signalling: pivoting around multiple phosphoinositide 3-kinases. Immunology **105**:125–136.
10. **Dairaghi, D. J., R. A. Fan, B. E. McMaster, M. R. Hanley, and T. J. Schall.** 1999. HHV8-encoded vMIP-I selectively engages chemokine receptor CCR8. Agonist and antagonist profiles of viral chemokines. J. Biol. Chem. **274**:21569–21574.
11. **Del Prete, G.** 1998. The concept of type-1 and type-2 helper T cells and their cytokines in humans. Int. Rev. Immunol. **16**:427–455.
12. **Dufva, M., J. Flodin, A. Nerstedt, U. Ruetschi, and L. Rymo.** 2002. Epstein-Barr virus nuclear antigen 5 inhibits pre-mRNA cleavage and polyadenylation. Nucleic Acids Res. **30**:2131–2143.
13. **Endres, M. J., C. G. Garlisi, H. Xiao, L. Shan, and J. A. Hedrick.** 1999. The Kaposi's sarcoma-related herpesvirus (KSHV)-encoded chemokine vMIP-I is a specific agonist for the CC chemokine receptor (CCR)8. J. Exp. Med. **189**:1993–1998.
14. **Finke, J., M. Rowe, B. Kallin, I. Ernberg, A. Rosen, J. Dillner, and G. Klein.** 1987. Monoclonal and polyclonal antibodies against Epstein-Barr virus nuclear antigen 5 (EBNA-5) detect multiple protein species in Burkitt's lymphoma and lymphoblastoid cell lines. J. Virol. **61**:3870–3878.
15. **Fleming, P., N. Davis-Poynter, M. Degli-Esposti, E. Densley, J. Papadimitriou, G. Shellam, and H. Farrell.** 1999. The murine cytomegalovirus chemokine homolog, m131/129, is a determinant of viral pathogenicity. J. Virol. **73**:6800–6809.
16. **Fu, Z., and M. J. Cannon.** 2000. Functional analysis of the $CD4^+$ T-cell response to Epstein-Barr virus: T-cell-mediated activation of resting B cells and induction of viral BZLF1 expression. J. Virol. **74**:6675–6679.
17. **Galfre, G., and C. Milstein.** 1981. Preparation of monoclonal antibodies: strategies and procedures. Methods Enzymol. **73**:3–46.
18. **Gonzalo, J. A., Y. Pan, C. M. Lloyd, G. Q. Jia, G. Yu, B. Dussault, C. A. Powers, A. E. Proudfoot, A. J. Coyle, D. Gearing, and J. C. Gutierrez-Ramos.** 1999. Mouse monocyte-derived chemokine is involved in airway hyperreactivity and lung inflammation. J. Immunol. **163**:403–411.
19. **Graham, G. J., L. Zhou, J. A. Weatherbee, M. L. Tsang, M. Napolitano, W. J. Leonard, and I. B. Pragnell.** 1993. Characterization of a receptor for macrophage inflammatory protein 1 alpha and related proteins on human and murine cells. Cell Growth Differ. **4**:137–146.
20. **Hammerschmidt, W., and B. Sugden.** 1989. Genetic analysis of immortalizing functions of Epstein-Barr virus in human B lymphocytes. Nature **340**: 393–397.
21. **Han, I., S. Harada, D. Weaver, Y. Xue, W. Lane, S. Orstavik, B. Skalhegg, and E. Kieff.** 2001. EBNA-LP associates with cellular proteins including DNA-PK and HA95. J. Virol. **75**:2475–2481.
22. **Han, I., Y. Xue, S. Harada, S. Orstavik, B. Skalhegg, and E. Kieff.** 2002. Protein kinase A associates with HA95 and affects transcriptional coactivation by Epstein-Barr virus nuclear proteins. Mol. Cell. Biol. **22**:2136–2146.
23. **Harada, S., and E. Kieff.** 1997. Epstein-Barr virus nuclear protein LP stimulates EBNA-2 acidic domain-mediated transcriptional activation. J. Virol. **71**:6611–6618.
24. **Igarashi, M., Y. Kawaguchi, K. Hirai, and F. Mizuno.** 2003. Physical interaction of Epstein-Barr virus (EBV) nuclear antigen leader protein (EBNA-LP) with human oestrogen-related receptor 1 (hERR1): hERR1 interacts with a conserved domain of EBNA-LP that is critical for EBV-induced B-cell immortalization. J. Gen. Virol. **84**:319–327.
25. **Imai, S., J. Nishikawa, and K. Takada.** 1998. Cell-to-cell contact as an efficient mode of Epstein-Barr virus infection of diverse human epithelial cells. J. Virol. **72**:4371–4378.
26. **Imai, S., M. Sugiura, O. Oikawa, S. Koizumi, M. Hirao, H. Kimura, H. Hayashibara, N. Terai, H. Tsutsumi, T. Oda, S. Chiba, and T. Osato.** 1996. Epstein-Barr virus (EBV)-carrying and -expressing T-cell lines established from severe chronic active EBV infection. Blood **87**:1446–1457.
27. **Imai, T., M. Baba, M. Nishimura, M. Kakizaki, S. Takagi, and O. Yoshie.** 1997. The T cell-directed CC chemokine TARC is a highly specific biological ligand for CC chemokine receptor 4. J. Biol. Chem. **272**:15036–15042.
28. **Imai, T., M. Nagira, S. Takagi, M. Kakizaki, M. Nishimura, J. Wang, P. W. Gray, K. Matsushima, and O. Yoshie.** 1999. Selective recruitment of CCR4-bearing Th2 cells toward antigen-presenting cells by the CC chemokines

thymus and activation-regulated chemokine and macrophage-derived chemokine. Int. Immunol. **11**:81–88.
29. **Imai, T., T. Yoshida, M. Baba, M. Nishimura, M. Kakizaki, and O. Yoshie.** 1996. Molecular cloning of a novel T cell-directed CC chemokine expressed in thymus by signal sequence trap using Epstein-Barr virus vector. J. Biol. Chem. **271**:21514–21521.
30. **Jeang, K. T., and S. D. Hayward.** 1983. Organization of the Epstein-Barr virus DNA molecule. III. Location of the P3HR-1 deletion junction and characterization of the *Not*I repeat units that form part of the template for an abundant 12-*O*-tetradecanoylphorbol-13-acetate-induced mRNA transcript. J. Virol. **48**:135–148.
31. **Jiang, W. Q., L. Szekely, V. Wendel-Hansen, N. Ringertz, G. Klein, and A. Rosen.** 1991. Co-localization of the retinoblastoma protein and the Epstein-Barr virus-encoded nuclear antigen EBNA-5. Exp. Cell Res. **197**:314–318.
32. **Kakinuma, T., K. Nakamura, M. Wakugawa, H. Mitsui, Y. Tada, H. Saeki, H. Torii, A. Asahina, N. Onai, K. Matsushima, and K. Tamaki.** 2001. Thymus and activation-regulated chemokine in atopic dermatitis: serum thymus and activation-regulated chemokine level is closely related with disease activity. J. Allergy Clin. Immunol. **107**:535–541.
33. **Kato, K. Y., A. Tobya, Y. Akashi, H. Nishiyama, and Y. Kawaguchi.** 2003. Identification of protein kinases responsible for phosphorylation of Epstein-Barr virus nuclear antigen leader protein at serine 35 that regulates its coactivator function. J. Gen. Virol. **84**:3381–3392.
34. **Kawaguchi, Y., and K. Kato.** 2003. Protein kinases conserved in herpesviruses potentially share a function mimicking the cellular protein kinase cdc2. Rev. Med. Virol. **13**:331–340.
35. **Kawaguchi, Y., K. Maeda, T. Miyazawa, M. Ono, C. Kai, and T. Mikami.** 1994. Nucleotide sequence and characterization of the feline herpesvirus type 1 immediate early gene. Virology **204**:430–435.
36. **Kawaguchi, Y., K. Nakajima, M. Igarashi, T. Morita, M. Tanaka, M. Suzuki, A. Yokoyama, G. Matsuda, K. Kato, M. Kanamori, and K. Hirai.** 2000. Interaction of Epstein-Barr virus nuclear antigen leader protein (EBNA-LP) with HS1-associated protein X-1: implication of cytoplasmic function of EBNA-LP. J. Virol. **74**:10104–10111.
37. **Kawaguchi, Y., C. Van Sant, and B. Roizman.** 1997. Herpes simplex virus 1 alpha regulatory protein ICP0 interacts with and stabilizes the cell cycle regulator cyclin D3. J. Virol. **71**:7328–7336.
38. **Kieff, E., and A. B. Rickinson.** 2001. Epstein-Barr virus and its replication, p. 2511–2573. *In* D. M. Knipe, P. M. Howley, D. E. Griffin, R. A. Lamb, M. A. Martin, B. Roizman, and S. E. Straus (ed.), Fields virology, 4th ed. Lippincott-Williams & Wilkins, Philadelphia, Pa.
39. **Kitay, M. K., and D. T. Rowe.** 1996. Protein-protein interactions between Epstein-Barr virus nuclear antigen-LP and cellular gene products: binding of 70-kilodalton heat shock proteins. Virology **220**:91–99.
40. **Lloyd, A. R., J. J. Oppenheim, D. J. Kelvin, and D. D. Taub.** 1996. Chemokines regulate T cell adherence to recombinant adhesion molecules and extracellular matrix proteins. J. Immunol. **156**:932–938.
41. **Mannick, J. B., J. I. Cohen, M. Birkenbach, A. Marchini, and E. Kieff.** 1991. The Epstein-Barr virus nuclear protein encoded by the leader of the EBNA RNAs is important in B-lymphocyte transformation. J. Virol. **65**:6826–6837.
42. **Mannick, J. B., X. Tong, A. Hemnes, and E. Kieff.** 1995. The Epstein-Barr virus nuclear antigen leader protein associates with hsp72/hsc73. J. Virol. **69**:8169–8172.
43. **Matsuda, G., K. Nakajima, Y. Kawaguchi, Y. Yamanashi, and K. Hirai.** 2003. Epstein-Barr virus (EBV) nuclear antigen leader protein (EBNA-LP) forms complexes with a cellular anti-apoptosis protein Bcl-2 or its EBV counterpart BHRF1 through HS1-associated protein X-1. Microbiol. Immunol. **47**:91–99.
44. **McCann, E. M., G. L. Kelly, A. B. Rickinson, and A. I. Bell.** 2001. Genetic analysis of the Epstein-Barr virus-coded leader protein EBNA-LP as a co-activator of EBNA2 function. J. Gen. Virol. **82**:3067–3079.
45. **Nakayama, T., R. Fujisawa, D. Izawa, K. Hieshima, K. Takada, and O. Yoshie.** 2002. Human B cells immortalized with Epstein-Barr virus upregulate CCR6 and CCR10 and downregulate CXCR4 and CXCR5. J. Virol. **76**:3072–3077.
46. **Nitsche, F., A. Bell, and A. Rickinson.** 1997. Epstein-Barr virus leader protein enhances EBNA-2-mediated transactivation of latent membrane protein 1 expression: a role for the W1W2 repeat domain. J. Virol. **71**:6619–6628.
47. **Pear, W. S., G. P. Nolan, M. L. Scott, and D. Baltimore.** 1993. Production of high-titer helper-free retroviruses by transient transfection. Proc. Natl. Acad. Sci. USA **90**:8392–8396.
48. **Pear, W. S., M. Scott, and G. P. Nolan.** 1997. Generation of high titer, helper-free retroviruses by transient transfection. Methods Mol. Med. **7**:41–57.
49. **Penfold, M. E., D. J. Dairaghi, G. M. Duke, N. Saederup, E. S. Mocarski, G. W. Kemble, and T. J. Schall.** 1999. Cytomegalovirus encodes a potent alpha chemokine. Proc. Natl. Acad. Sci. USA **96**:9839–9844.
50. **Peng, R., A. V. Gordadze, E. M. Fuentes Panana, F. Wang, J. Zong, G. S. Hayward, J. Tan, and P. D. Ling.** 2000. Sequence and functional analysis of EBNA-LP and EBNA2 proteins from nonhuman primate lymphocryptoviruses. J. Virol. **74**:379–389.
51. **Rickinson, A. B., and E. Kieff.** 2001. Epstein-Barr virus. p. 2575–2627. *In* D. M. Knipe, P. M. Howley, D. E. Griffin, R. A. Lamb, M. A. Martin, B. Roizman, and S. E. Straus (ed.), Fields virology, 4th ed. Lippincott-Williams & Wilkins, Philadelphia, Pa.
52. **Romagnani, S.** 1994. Lymphokine production by human T cells in disease states. Annu. Rev. Immunol. **12**:227–257.
53. **Saederup, N., Y. C. Lin, D. J. Dairaghi, T. J. Schall, and E. S. Mocarski.** 1999. Cytomegalovirus-encoded beta chemokine promotes monocyte-associated viremia in the host. Proc. Natl. Acad. Sci. USA **96**:10881–10886.
54. **Sample, J., M. Hummel, D. Braun, M. Birkenbach, and E. Kieff.** 1986. Nucleotide sequences of mRNAs encoding Epstein-Barr virus nuclear proteins: a probable transcriptional initiation site. Proc. Natl. Acad. Sci. USA **83**:5096–5100.
55. **Sekiya, T., M. Miyamasu, M. Imanishi, H. Yamada, T. Nakajima, M. Yamaguchi, T. Fujisawa, R. Pawankar, Y. Sano, K. Ohta, A. Ishii, Y. Morita, K. Yamamoto, K. Matsushima, O. Yoshie, and K. Hirai.** 2000. Inducible expression of a Th2-type CC chemokine thymus- and activation-regulated chemokine by human bronchial epithelial cells. J. Immunol. **165**:2205–2213.
56. **Sekiya, T., H. Yamada, M. Yamaguchi, K. Yamamoto, A. Ishii, O. Yoshie, Y. Sano, A. Morita, K. Matsushima, and K. Hirai.** 2002. Increased levels of a TH2-type CC chemokine thymus and activation-regulated chemokine (TARC) in serum and induced sputum of asthmatics. Allergy **57**:173–177.
57. **Shimizu, N., H. Yoshiyama, and K. Takada.** 1996. Clonal propagation of Epstein-Barr virus (EBV) recombinants in EBV-negative Akata cells. J. Virol. **70**:7260–7263.
58. **Sinclair, A. J., I. Palmero, G. Peters, and P. J. Farrell.** 1994. EBNA-2 and EBNA-LP cooperate to cause G0 to G1 transition during immortalization of resting human B lymphocytes by Epstein-Barr virus. EMBO J. **13**:3321–3328.
59. **Sozzani, S., W. Luini, G. Bianchi, P. Allavena, T. N. Wells, M. Napolitano, G. Bernardini, A. Vecchi, D. D'Ambrosio, D. Mazzeo, F. Sinigaglia, A. Santoni, E. Maggi, S. Romagnani, and A. Mantovani.** 1998. The viral chemokine macrophage inflammatory protein-II is a selective Th2 chemoattractant. Blood **92**:4036–4039.
60. **Stine, J. T., C. Wood, M. Hill, A. Epp, C. J. Raport, V. L. Schweickart, Y. Endo, T. Sasaki, G. Simmons, C. Boshoff, P. Clapham, Y. Chang, P. Moore, P. W. Gray, and D. Chantry.** 2000. KSHV-encoded CC chemokine vMIP-III is a CCR4 agonist, stimulates angiogenesis, and selectively chemoattracts TH2 cells. Blood **95**:1151–1157.
61. **Strieter, R. M., P. J. Polverini, D. A. Arenberg, and S. L. Kunkel.** 1995. The role of CXC chemokines as regulators of angiogenesis. Shock **4**:155–160.
62. **Szekely, L., W. Q. Jiang, K. Pokrovskaja, K. G. Wiman, G. Klein, and N. Ringertz.** 1995. Reversible nucleolar translocation of Epstein-Barr virus-encoded EBNA-5 and hsp70 proteins after exposure to heat shock or cell density congestion. J. Gen. Virol. **76**:2423–2432.
63. **Szekely, L., K. Pokrovskaja, W. Q. Jiang, H. de The, N. Ringertz, and G. Klein.** 1996. The Epstein-Barr virus-encoded nuclear antigen EBNA-5 accumulates in PML-containing bodies. J. Virol. **70**:2562–2568.
64. **Szekely, L., G. Selivanova, K. P. Magnusson, G. Klein, and K. G. Wiman.** 1993. EBNA-5, an Epstein-Barr virus-encoded nuclear antigen, binds to the retinoblastoma and p53 proteins. Proc. Natl. Acad. Sci. USA **90**:5455–5459.
65. **Tanaka, M., H. Kagawa, Y. Yamanashi, T. Sata, and Y. Kawaguchi.** 2003. Construction of an excisable bacterial artificial chromosome containing a full-length infectious clone of herpes simplex virus type 1: viruses reconstituted from the clone exhibit wild-type properties in vitro and in vivo. J. Virol. **77**:1382–1391.
66. **Tanaka, M., Y. Kawaguchi, J. Yokofujita, M. Takagi, Y. Eishi, and K. Hirai.** 1999. Sequence variations of Epstein-Barr virus LMP2A gene in gastric carcinoma in Japan. Virus Genes **19**:103–111.
67. **Tanaka, M., A. Yokoyama, M. Igarashi, G. Matsuda, K. Kato, M. Kanamori, K. Hirai, Y. Kawaguchi, and Y. Yamanashi.** 2002. Conserved region CR2 of Epstein-Barr virus nuclear antigen leader protein is a multifunctional domain that mediates self-association as well as nuclear localization and nuclear matrix association. J. Virol. **76**:1025–1032.
68. **Tanaka, Y., D. H. Adams, S. Hubscher, H. Hirano, U. Siebenlist, and S. Shaw.** 1993. T-cell adhesion induced by proteoglycan-immobilized cytokine MIP-1 beta. Nature **361**:79–82.
69. **Van Snick, J., F. Houssiau, P. Proost, J. Van Damme, and J. C. Renauld.** 1996. I-309/T cell activation gene-3 chemokine protects murine T cell lymphomas against dexamethasone-induced apoptosis. J. Immunol. **157**:2570–2576.
70. **Veronese, M. L., A. Veronesi, E. D'Andrea, A. Del Mistro, S. Indraccolo, M. R. Mazza, M. Mion, R. Zamarchi, C. Menin, M. Panozzo, et al.** 1992. Lymphoproliferative disease in human peripheral blood mononuclear cell-injected SCID mice. I. T lymphocyte requirement for B cell tumor generation. J. Exp. Med. **176**:1763–1767.
71. **Vestergaard, C., H. Yoneyama, M. Murai, K. Nakamura, K. Tamaki, Y. Terashima, T. Imai, O. Yoshie, T. Irimura, H. Mizutani, and K. Matsushima.** 1999. Overproduction of Th2-specific chemokines in NC/Nga mice exhibiting atopic dermatitis-like lesions. J. Clin. Investig. **104**:1097–1105.
72. **Wong, M. M., and E. N. Fish.** 2003. Chemokines: attractive mediators of the immune response. Semin. Immunol. **15**:5–14.
73. **Yokoyama, A., Y. Kawaguchi, I. Kitabayashi, M. Ohki, and K. Hirai.** 2001.

The conserved domain CR2 of Epstein-Barr virus nuclear antigen leader protein is responsible not only for nuclear matrix association but also for nuclear localization. Virology **279:**401–413.

74. **Yokoyama, A., M. Tanaka, G. Matsuda, K. Kato, M. Kanamori, H. Kawasaki, H. Hirano, I. Kitabayashi, M. Ohki, K. Hirai, and Y. Kawaguchi.** 2001. Identification of major phosphorylation sites of Epstein-Barr virus nuclear antigen leader protein (EBNA-LP): ability of EBNA-LP to induce latent membrane protein 1 cooperatively with EBNA-2 is regulated by phosphorylation. J. Virol. **75:**5119–5128.
75. **Zou, P., Y. Isegawa, K. Nakano, M. Haque, Y. Horiguchi, and K. Yamanishi.** 1999. Human herpesvirus 6 open reading frame U83 encodes a functional chemokine. J. Virol. **73:**5926–5933.

American Journal of Pathology, Vol. 163, No. 6, December 2003

Short Communication

A Tetraspanin-Family Protein, T-Cell Acute Lymphoblastic Leukemia-Associated Antigen 1, Is Induced by the Ewing's Sarcoma-Wilms' Tumor 1 Fusion Protein of Desmoplastic Small Round-Cell Tumor

Emi Ito,*† Reiko Honma,*† Jun-ichi Imai,* Sakura Azuma,‡ Takayuki Kanno,§ Shigeo Mori,§ Osamu Yoshie,¶ Jun Nishio,‖ Hiroshi Iwasaki,‖ Koichi Yoshida,** Jin Gohda,‡ Jun-ichiro Inoue,‡ Shinya Watanabe,* and Kentaro Semba‡

From the Division of Cancer Genomics, the Division of Cellular and Molecular Biology,‡ and the Division of Pathology,¶ Department of Cancer Biology, The Institute of Medical Science, The University of Tokyo, Tokyo; Japan Biological Informatics Consortium,† Hacchobori, Tokyo; the Department of Microbiology,¶ Kinki University School of Medicine, Osaka-Sayama, Osaka; the Department of Pathology,‖ School of Medicine, Fukuoka University, Fukuoka; and the Department of Biology,** School of Medicine, Sapporo Medical University, Chuo-ku, Sapporo, Japan*

Recurrent chromosomal translocations in neoplasms often generate hybrid genes that play critical roles in tumorigenesis. Desmoplastic small round-cell tumor (DSRCT) is an aggressive malignancy associated with the chromosomal translocation t(11;22)(p13;q12). This translocation generates a chimeric transcription factor, EWS-WT1, which consists of the transcriptional activation domain of the Ewing's sarcoma (EWS) protein and the DNA binding domain of the Wilms' tumor 1 (WT1) protein. One of the splice variants, EWS-WT1(-KTS) lacks three amino acid residues (Lys-Thr-Ser) in the DNA binding domain and transforms NIH3T3 cells. Therefore, it is likely that aberrant gene expression caused by EWS-WT1(-KTS) is involved in the malignant phenotype of DSRCT. Microarray analysis of 9600 human genes revealed that a gene encoding a tetraspanin-family protein, T-cell acute lymphoblastic leukemia-associated antigen 1 (TALLA-1), was induced in EWS-WT1(-KTS)-expressing cell clones. This induction was EWS-WT1(-KTS)-specific, and more importantly, TALLA-1 protein was expressed in the three independent cases of DSRCT. Tetraspanin-family genes encode transmembrane proteins that regulate various cell processes such as cell adhesion, migration and metastasis. Our findings provide a novel insight into the malignant phenotype of DSRCT, suggesting that TALLA-1 is a useful marker for diagnosis and a potential target for the therapy of DSRCT. ***(Am J Pathol 2003, 163:2165–2172)***

Specific recurrent chromosomal translocation in malignant tumors is thought to play a causative role in tumorigenesis. Translocation frequently generates a chimeric gene, and the functions of such chimeric genes have been studied extensively to clarify the molecular mechanisms underlying tumorigenesis. Desmoplastic small round-cell tumor (DSRCT) is an aggressive neoplasm with distinctive histological and immunophenotypic features that suggest a multilineage origin.[1–3] The tumor often develops in the abdominal and pelvic peritoneum of adolescent males. Recent integrated strategies including surgery, multiagent chemotherapy, and radiation therapy have improved the prognosis considerably, although progression-free survival remains poor.[3] Thus, identification of tumor-associated antigens for DSRCT would be useful for the development of anti-tumor drugs. DSRCT has a unique chromosomal translocation t(11;22)(p13;q12) that

Supported by a Grant-in-Aid for Scientific Research from the Ministry of Education, Culture, Sports, Science and Technology of Japan and by a grant from the New Energy and Industrial Technology Development Organization (NEDO).

Accepted for publication August 28, 2003.

Address reprint requests to Kentaro Semba, Ph.D., Division of Cellular and Molecular Biology, Department of Cancer Biology, The Institute of Medical Science, The University of Tokyo, 4-6-1 Shirokanedai, Minato-ku, Tokyo 108-8639, Japan. E-mail: ksemba@ims.u-tokyo.ac.jp.

generates a chimeric gene comprising part of the *Ewing's sarcoma* (*EWS*) gene on chromosome 22 and the *Wilms' tumor 1* (*WT1*) gene on chromosome 11.[4,5] The EWS-WT1 chimeric protein consists of the N-terminal transcriptional regulatory domain of EWS and the C-terminal three zinc-finger motifs of WT1 as the DNA binding domain. Therefore, the fusion protein acts as a transcriptional activator. Alternative splicing in the *WT1* region generates two types of EWS-WT1 protein. One isoform, EWS-WT1(-KTS), which lacks three amino acid residues (Lys-Thr-Ser) between the third and the fourth zinc fingers of WT1, confers NIH3T3 cells with anchorage-independent growth and tumorigenicity in nude mice.[6] In contrast, EWS-WT1(+KTS), which contains the three amino acid residues, does not have such transforming activity. Thus, the EWS-WT1 protein is a molecular marker for DSRCT and is believed to be involved in tumorigenesis.

Recent reports have shown that EWS-WT1(-KTS) activates a number of genes, including those encoding platelet-derived growth factor-A,[7] insulin-like growth factor-1 receptor,[8,9] interleukin-2/15 receptor β-chain (IL2/15Rβ),[10] and brain-specific angiogenesis inhibitor 1-associated protein 3 (BAIAP3).[11] In the present study, we used DNA microarrays to carry out a comprehensive analysis of the downstream genes that are up-regulated by EWS-WT1(-KTS). We found that a tetraspanin-family protein, T-cell acute lymphoblastic leukemia-associated antigen 1 (TALLA-1, also referred to as A15,[12] CCG-B7,[13] and TM4SF2), was induced specifically by EWS-WT1(-KTS) and TALLA1 protein was expressed in the three independent cases of DSRCT. Tetraspanin-family proteins contain four transmembrane domains and two extracellular loops. This evolutionally conserved gene family contains more than 30 known members in mammals, 37 in *Drosophila* and 20 in *Caenorhabditis elegans*.[14] They regulate a variety of normal and pathological processes such as cell adhesion, motility, egg-sperm fusion, virus-induced syncytium formation, and cancer metastasis through formation of a network of multimolecular complexes via tetraspanin-tetraspanin and tetraspanin-protein interactions.[14,15] We discuss the significance of TALLA-1 in the malignant phenotype of tumors.

Materials and Methods

Microarray Analysis

Synthetic polynucleotides (80-mers) representing 9600 human genes (MicroDiagnostic, Tokyo, Japan) were arrayed with a custom-made arrayer. Poly(A)$^+$ RNA was prepared from cells with TRIzol reagent (Invitrogen, Carlsbad, CA) and Poly(A)Purist Kit (Ambion, Austin, TX). Two micrograms of poly(A)$^+$ RNA were labeled with Cyanine 5-dUTP or Cyanine 3-dUTP. Hybridization and subsequent washes of arrays were performed with a Labeling & Hybridization Kit (MicroDiagnostic). Hybridization signals were measured with a GenePix 400A scanner (Axon Instruments, Union City, CA) and then processed into primary expression ratios (ratios of Cyanine 5-labeled to Cyanine 3-labeled samples) by the GenePix Pro software (Axon Instruments). A secondary ratio of expression of each gene was calculated by averaging the primary expression ratio obtained from an experiment with Cyanine 5-labeled target and Cyanine 3-labeled control sample and the reciprocal of the primary expression ratio obtained from an experiment with Cyanine 5-labeled control and Cyanine 3-labeled target. The secondary expression ratios calculated from the pair of experiments were converted into $\log_2$ values as the final expression ratios.

Cells

A human osteosarcoma cell line, U2OS, was maintained in Dulbecco's modified Eagle's medium (DMEM) with 10% fetal bovine serum (FBS). A human DSRCT cell line, JN-DSRCT-1,[16] was maintained in DMEM:Nutrient Mixture F12 (1:1) mixture with 10% FBS. To establish clones with stable expression of EWS-WT1(-KTS), U2OS cells (1×10^5) were transfected with 2 μg of an EWS-WT1(-KTS) expression vector, pcDNA-EWS-WT1(-KTS), and 6 μl of Lipofectamine (Invitrogen). Clones were isolated in the presence of 800 μg/ml of G418 and used for subsequent microarray analysis. A mixture of mock-transfected cells was maintained in the presence of G418 and used as control.

Transfection

A nucleofector device (Amaxa Biosystems, Cologne, Germany) was used for highly efficient gene transfer. This device delivers DNA directly into nuclei, allowing exogenous gene expression after a short incubation period of only 2 to 8 hours. U2OS cells (2×10^6) were transfected with 2 μg of an expression vector with R solution and the pre-set U-16 program. The transfection efficiency was monitored by flow cytometric analysis of pCMV-GFP transfected cells.

Western Blotting

Proteins solubilized in Laemmli sample buffer were resolved on 10% sodium dodecyl sulfate (SDS)-polyacrylamide gels and blotted onto Immobilon membranes (Millipore Co., Bedford, MA). Filters were probed for WT1 and EWS-WT1 with anti-WT1 antibody (C19; Santa Cruz Biotechnology, Inc., Santa Cruz, CA) and for EWS-FLI1 with anti-FLI1 antibody (C19; Santa Cruz Biotechnology). Bands were visualized with Renaissance Chemiluminescence Reagent Plus (NEN Life Sci Products, Boston, MA).

Reverse Transcription-Polymerase Chain Reaction (RT-PCR)

RNA was prepared with TRIzol reagent from cultured cells or tumor tissues. First-strand cDNA was synthesized using SuperScript first-strand synthesis system for RT-PCR (Invitrogen). *Taq* polymerase was purchased from Sigma (St. Louis, MO). Primers are 5′-TACACGGACGCTATG-CAGAC-3′ and 5′-GATTCCAAACGCCACTCCAG-3′ for

Talla-1, 5′-TACCCCATGCAGCCAGTCAC-3′ and 5′-TTTGAGCTGGTCTGAACGAG-3′ for *EWS-WT1*, and 5′-CCAGCCGAGCCACATCGCTC-3′ and 5′-ATGAGCCCCAGCCTTCTCCAT-3′ for *GAPDH*.

Northern Blotting

Northern blotting was done with the NorthernMax Kit (Ambion). ^{32}P-labeled probe was prepared with a Multiprime DNA Labeling System (Amersham Biosciences, Arlington Heights, IL).

Flow Cytometry

Cells were incubated with ascites diluted 100-fold containing monoclonal anti-TALLA-1 antibody (B2D) and fluorescent anti-mouse IgG (Alexa Fluor 488; Molecular Probes, Eugene, OR), and then subjected to flow cytometric analysis (Epics XL; Beckman Coulter, Fullerton, CA).

Immunofluorescence

Cells seeded on cover glasses were fixed with 4% paraformaldehyde for 15 minutes at 37°C, and permeabilized with 0.2% Triton X-100/PBS for 5 minutes at room temperature. EWS-WT1 and TALLA-1 were detected with the same antibodies diluted 100-fold as used for Western blotting and flow cytometry. Proteins were visualized with fluorescent secondary antibody (Molecular Probes).

Immunohistochemistry

Frozen blocks and sections of DSRCT were kindly provided by the Pediatric Division of Cooperative Human Tissue Network (Columbus, OH). Diagnosis of DSRCT was confirmed on hematoxylin and eosin-stained frozen sections by pathologists T. K. and S. M. For detection of TALLA-1, frozen sections were incubated with 800-fold diluted B2D and then subjected to color reaction with the indirect immunoperoxidase method (Histofine Simple Stain, Nichirei, Japan).

Results

To explore comprehensively downstream genes with expression induced by EWS-WT1(-KTS), we established three clonal lines of U2OS cells that stably expressed EWS-WT1(-KTS). Microarray analysis of 9600 human genes identified a group of genes whose expression was reproducibly induced or repressed in these clones (Table 1). These genes included those encoding IL2/15Rβ, adrenomedullin, and BAIAP3, which were reported previously.[10,11] We also found that expression of desmin, an established molecular marker for DSRCT, was induced by EWS-WT1(-KTS). We confirmed the change in expression of desmin by immunoblotting (data not shown).

We also found that expression of *Talla-1*, a member of the tetraspanin family and a marker of T-cell acute lymphoblastic leukemia (T-ALL),[17] was up-regulated in clones expressing EWS-WT1(-KTS). Northern blotting confirmed the induction of *Talla-1* mRNA in the clones (C9 and D9; Figure 1A). Flow cytometric analysis showed that TALLA-1 protein was expressed on the plasma membranes of EWS-WT1(-KTS)-expressing cells (Figure 1B). To exclude the possibility that these changes reflected clonal variation, we analyzed *Talla-1* expression in cells that transiently expressed EWS-WT1(-KTS). For this purpose, we used a Nucleofector device, which enabled us to achieve approximately 80% transfection efficiency. EWS-WT1(-KTS) protein was detected at 8 hours after transfection, was sustained at 24 hours, and then gradually decreased (Figure 2A). With transient transfection, *Talla-1* mRNA was initially detected at 8 hours, and was expressed at high levels at 24 hours after transfection of vector encoding EWS-WT1(-KTS) (Figure 2A). To examine if the induction of *Talla-1* expression is specific to EWS-WT1(-KTS), we transfected vectors encoding EWS-WT1(+KTS), EWS-FLI1, WT1(-KTS), and WT1(+KTS) into U2OS cells. EWS-FLI1 is generated by chromosomal translocation t(11;22)(q24;q12), and is found in 85% of cases of Ewing's sarcoma. The fusion protein consists of the N-terminal transcriptional activation domain of EWS and the C-terminal ETS DNA binding domain of FLI1. Thus, the primary target genes of Ewing's sarcoma are thought to be different from those of DSRCT because of the difference in DNA recognition. Northern blot analysis revealed that only EWS-WT1(-KTS) induced *Talla-1* expression (Figure 2B).

Recently a DSRCT cell line, JN-DSRCT-1, was established from the pleural effusion of a patient with pulmonary metastasis from a typical intraabdominal DSRCT.[16] We confirmed that *Talla-1* mRNA and protein were expressed in this cell line (data not shown). Because some tetraspanins are localized not only on the plasma membrane but also at the intracellular compartments such as lysosome and exosome, we analyzed subcellular localization of TALLA-1 by immunohistochemistry. Figure 2C shows that TALLA-1 protein in U2OS cells was also localized in the cytoplasm when cells were permeabilized. This dot-like localization pattern is quite similar to that of endogenous TALLA-1 in JN-DSRCT-1 cells. Induction of *Talla-1* mRNA was also observed when the EWS-WT1(-KTS) expression vector was transfected into human 293T cells, indicating that induction of *Talla-1* expression by EWS-WT1(-KTS) was not specific to U2OS cells (data not shown). Taken together, these data suggest that EWS-WT1(-KTS) induces expression of *Talla-1* mRNA and protein in human cells without cell type-specific cofactors.

We then examined expression of TALLA-1 in DSRCT specimens. Because the supply and amount of tumor tissues were limited, we used RT-PCR analysis to detect *Talla-1* mRNA. Under the condition we used, *Talla-1* mRNA was detected in three of three independent DSRCT tissues (Figure 3A). Immunohistochemical analysis showed localization of TALLA-1 protein in the nest of tumor cells in all three specimens (representative data shown in Figure 3B). Less intense reaction was noted on the stromal endothelial cells. Other cellular components including fibroblasts, lymphocytes, fat cells, myothelial cells, or adventitial cells were basically unstained.

Table 1. Microarray Identification of Genes Activated or Repressed Downstream of EWS-WT1(-KTS)

Gene symbol	Accession number	B12	C9	D9	Average
RGS5	NM_003617	4.8069	4.5771	4.9195	4.7678
DKFZp434B227	NM_032263	4.3451	4.6415	4.9425	4.6430
DES (desmin)	NM_001927	4.8052	3.3748	5.1433	4.4411
APOA1	NM_000039	3.4595	5.0025	3.7444	4.0688
CHI3L1	NM_001276	3.4901	4.4559	3.8189	3.9216
WT1	NM_024424	3.9531	3.8653	3.8197	3.8794
NK4	NM_004221	2.7691	4.3032	4.1529	3.7417
APOL2	NM_030882	3.5625	4.3115	2.9113	3.5951
FLJ20245	NM_017723	3.4295	3.6399	2.9387	3.3360
ADM (adrenomedullin)	NM_001124	3.2513	4.1579	2.4834	3.2975
LOC135562	XM_069429	3.0812	4.5899	2.0095	3.2269
BAIAP3	NM_003933	2.6486	4.0179	2.6717	3.1127
BIK	NM_001197	2.3391	3.4097	3.3323	3.0270
LOC90189	XM_029748	2.9116	2.7470	2.8376	2.8321
FLJ22671	NM_024861	2.4854	2.7474	3.1525	2.7951
KLK6	NM_002774	2.8500	2.5292	2.7768	2.7187
LCK	NM_005356	1.7054	2.2152	4.1992	2.7066
IL8	NM_000584	1.9838	3.7999	2.2517	2.6785
DRP2	NM_001939	1.9726	2.7053	3.2519	2.6433
KREMEN2	NM_024507	2.3643	2.9575	2.3405	2.5541
TNFRSF21	NM_014452	2.3449	2.9221	2.2719	2.5130
SSTR3	NM_001051	2.7267	2.5529	2.1279	2.4692
FLJ20154	NM_017787	1.8621	2.3683	2.9680	2.3995
NFATC1	NM_006162	2.3952	2.8337	1.9534	2.3941
GAGE7	NM_021123	3.0143	2.0046	2.1603	2.3931
SNX9	NM_016224	2.3430	2.3643	2.2830	2.3301
TM4SF2 (Talla-1)	NM_004615	1.8004	2.4611	2.6285	2.2967
LOC139728	XM_060051	2.2622	2.3246	2.1933	2.2600
TRIM29	NM_012101	2.0576	2.8573	1.8001	2.2383
SERPINB2	NM_002575	2.1313	2.2954	2.2759	2.2342
RELB	NM_006509	1.9808	2.8510	1.8384	2.2234
FLJ23058	NM_024696	2.1799	1.9497	2.5029	2.2108
IL2RB (IL2 receptor β)	NM_000878	2.4299	2.5900	1.5083	2.1761
HSPC022	NM_014029	2.2705	2.4120	1.8273	2.1699
MSLN	NM_005823	1.9397	2.2261	2.2971	2.1543
OPRL1	NM_000913	1.9394	2.7325	1.5796	2.0838
MAGP2	NM_003480	2.3341	2.0496	1.6075	1.9971
NEDD4L	NM_015277	1.7847	2.4666	1.7302	1.9938
SLC2A3	NM_006931	1.6088	2.2489	2.1073	1.9883
BGN	NM_001711	1.5921	1.9808	2.3423	1.9717
COL6A3	NM_004369	1.8971	2.3618	1.5310	1.9300
S100A4	NM_002961	1.8033	2.2082	1.6691	1.8935
KRT17	NM_000422	1.6139	2.2038	1.6792	1.8323
MS4A6A	NM_022349	1.7096	2.0112	1.5267	1.7492
C18orf1	NM_004338	−1.5796	−1.5385	−1.6386	−1.5856
H1F2	NM_005319	−1.9450	−1.7604	−1.8163	−1.8406
OSBPL10	NM_017784	−1.6272	−2.2958	−1.6578	−1.8603
FXYD6	NM_022003	−1.5180	−2.1517	−1.9351	−1.8683
HNOEL-iso	NM_020190	−1.8806	−2.7950	−1.5057	−2.0604
P311	NM_004772	−2.0767	−2.2441	−1.9064	−2.0757
NECL1	NM_021189	−1.5862	−3.3417	−1.9093	−2.2791
FLJ20716	NM_017938	−2.0441	−2.7866	−2.2385	−2.3564
H2AFL	NM_003512	−2.4452	−2.2226	−2.4156	−2.3611
BRAK	NM_004887	−2.2034	−2.7810	−2.4533	−2.4792
CRTL1	NM_001884	−1.9105	−3.5013	−2.0543	−2.4887
SERPINF1	NM_002615	−1.8785	−3.0730	−2.6775	−2.5430
MMP2	NM_004530	−2.4785	−2.8093	−2.4158	−2.5679
LOC51316	NM_016619	−2.7566	−3.4258	−2.2395	−2.8073
SRCRB4D	NM_080744	−3.4141	−3.1876	−3.4979	−3.3665
MVD	NM_002461	−3.1784	−3.7718	−3.9392	−3.6298

Expression levels ($\log_2$ values) of 9,600 human genes in the three EWS-WT1(-KTS)-expressing U2OS clones (B12, C9, and D9) relative to a mixture of control mock-transfected clones are calculated as expression ratios processed from the raw data of two individual experiments labeled reciprocally with two different fluors. Genes listed in the table show more or less than 1.5 of expression level ($\log_2$ values) in all three clones. A more detailed description of each gene is available on the National Center for Biotechnology Information website (http://www.ncbi.nlm.nih.gov/).

Discussion

In the present study, we screened for downstream genes with expression induced by EWS-WT1(-KTS), which is thought to be involved in the tumorigenesis of DSRCT. The overall profile of gene expression by EWS-WT1(-KTS)-expressing cells was quite different from that of WT1(-KTS)-expressing cells (Ito E, unpublished data). In addition to the replacement of transcriptional regulatory domain of WT1 with that of EWS, the N-terminal first zinc finger that contributes to the binding specificity of WT1 is deleted

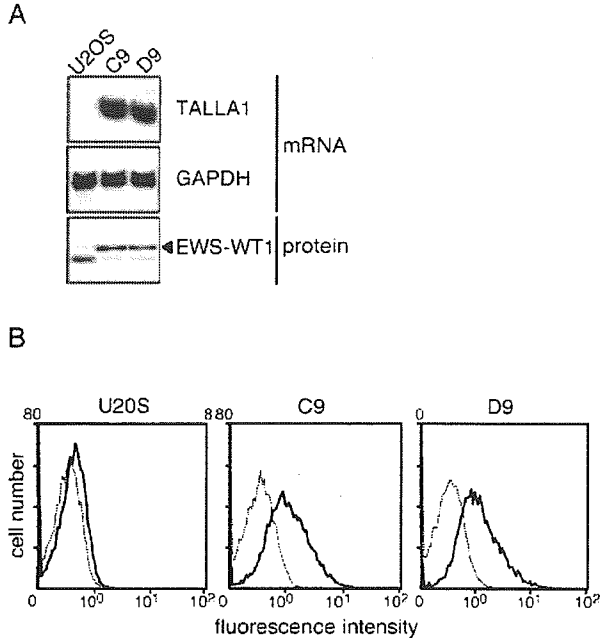

Figure 1. Expression of *Talla-1* in cell clones stably expressing EWS-WT1(-KTS). **A:** Northern blotting analysis of *Talla-1* mRNA. Total RNA (5 μg) was loaded in each lane. EWS-WT1(-KTS) protein (**filled triangle**) was detected by Western blotting with anti-WT1 antibody. **B:** Flow cytometric analysis of TALLA-1 protein. Living cells were incubated with anti-TALLA-1 (B2D) monoclonal antibody and Alexa-Fluor 488-labeled anti-mouse IgG and then subjected to flow cytometric analysis (**solid line**). Background profiles (**dotted line**) were measured by staining with Alexa-Fluor 488-labeled anti-mouse IgG only.

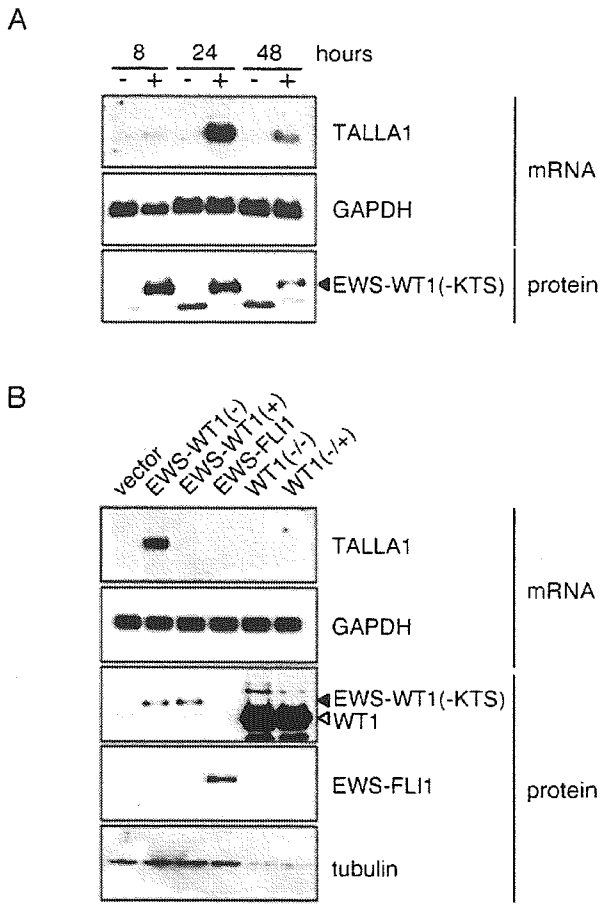

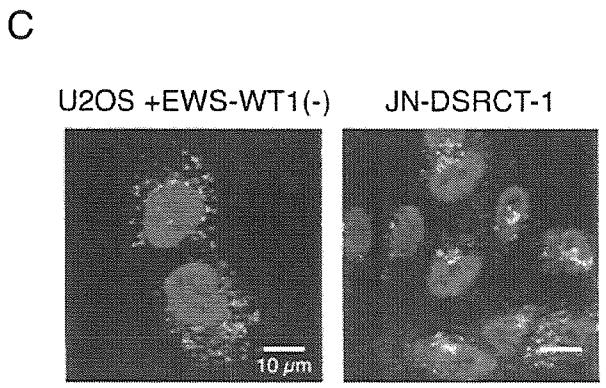

Figure 2. Specific expression of *Talla-1* mRNA and subcellular localization of TALLA-1 protein in cells transiently expressing EWS-WT1(-KTS). **A:** Time course of *Talla-1* mRNA induction after transfection of vector encoding EWS-WT1(-KTS). RNA and protein were prepared at the indicated times after transfection. **B:** Specific induction of *Talla-1* expression by EWS-WT1(-KTS). Each expression vector was introduced into U2OS cells and then RNA and protein were prepared 24 hours after transfection. **C:** Immunofluorescent staining of EWS-WT1(-KTS)-transfected cells and JN-DSRCT-1. TALLA-1 and EWS-WT1 were stained with Alexa Fluor 488 (green) and Alexa Fluor 568 (red), respectively.

during the generation of the EWS-WT1 fusion protein.[18,19] Moreover, EWS-WT1 has 10-times higher binding affinity for WT1-binding sequence than WT1.[20] Such differences may account for the unique expression profile of EWS-WT1.

We found that *Talla-1*, a member of the tetraspanin family, was expressed in a DSRCT cell line and tumor specimens, and was induced specifically by EWS-WT1(-KTS). Transcriptional regulatory sequence of the *Talla-1* gene has not been identified so far; thus, mechanism of *Talla-1* induction by EWS-WT1(-KTS) remains to be analyzed. *Talla-1* was initially identified due to its preferential expression in T-ALL and neuroblastoma cell lines[12,17] In addition, *Talla-1* is expressed at high levels in neurons of the brain,[21] and intriguingly its inactivation by chromosomal translocation (X;2) or by point mutations (Gly218 to stop codon, Pro172 to His) is associated with X-linked forms of nonsyndromic mental retardation (MRX).[22] Aberrant expression of *Talla-1* in T-ALL is mediated cooperatively by two transcription factors, TAL1 and RBTN1, both of which are ectopically activated by chromosomal translocation in T-ALL,[23] thus *Talla-1* may be a common target that is involved in oncogenesis. The biochemical and biological function of TALLA-1 is largely unknown except that TALLA-1 is associated with phosphoinositide 4-kinase.[24] Accumulating evidence indicate that tetraspanin proteins regulate integrin-extracellular matrix (ECM) interaction,[25] which includes migration,[26] invasion into collagen gels,[27] and morphology on Matrigel.[28] Furthermore, ligation of tetraspanin-α3β1 integrin complex by anti-tetraspanin or anti-integrin antibodies induces phosphoinositide 3-kinase-dependent production of matrix metalloproteinase 2 (MMP2) and long invasive protrusions within Matrigel, which is thought to increase invasive potential of tumor cells in the three

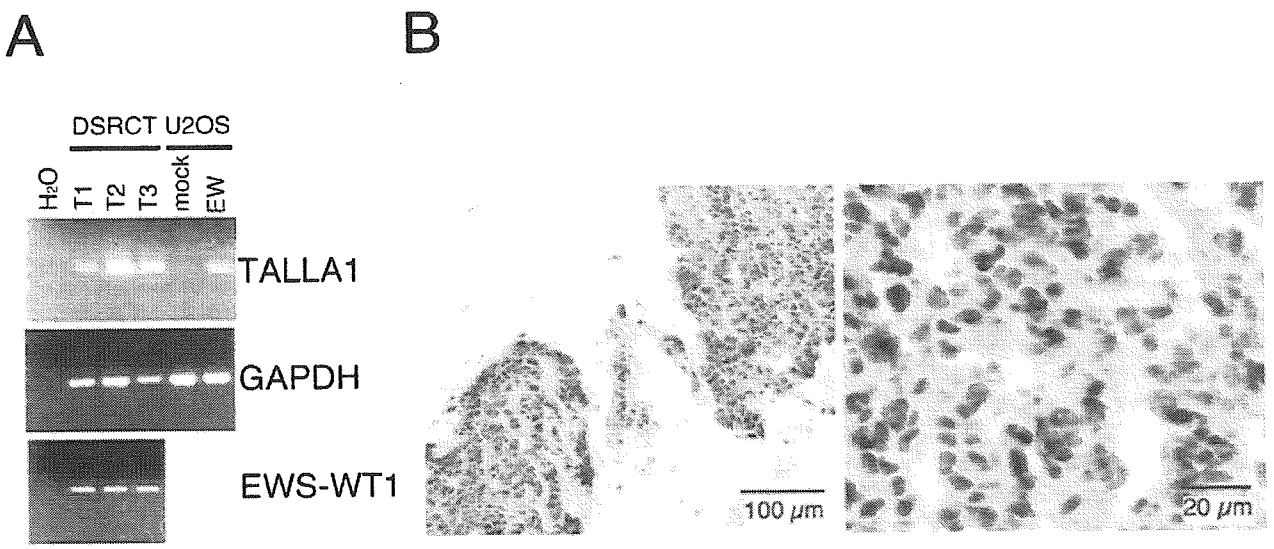

Figure 3. Expression of TALLA-1 in DSRCT specimens. **A:** RT-PCR analysis of the *Talla-1* mRNA in DSRCT. The *Talla-1* mRNA was amplified from various sources by RT-PCR and then separated by electrophoresis on agarose gels. Sources are DSRCT tissues (T1, T2, T3), cells transiently expressing EWS-WT1(-KTS) (EW) or its negative control (mock), and various human tissues. Expression of *EWS-WT1* fusion transcript was also detected in the three DSRCT tumors. PCR products were visualized by staining with ethidium bromide and UV transillumination. **B:** Immunohistochemical staining of a DSRCT specimen (T3). TALLA-1-positive cells are stained brown. Sections were counter-stained with hematoxylin.

dimensional extracellular matrix environment.[29] Recent biomechanical analysis directly showed that CD151, a member of the tetraspanin family, selectively strengthens $\alpha 6\beta 1$ integrin-mediated adhesion to laminin-1.[30] Exogenous expression of tetraspanin proteins, Co-029 and CD151, increases the metastatic potentials of tumor cell lines[31,32] and anti-CD151 antibody inhibits metastasis and migration of a CD151-expressing tumor cell line.[31] Taken together, TALLA-1 may be involved in cellular processes, including cell adhesion and regulation of cytoskeleton through a phosphoinositide-dependent signaling pathway, which may reflect infiltration and desmoplastic character of DSRCT. This hypothesis is also attractive for pathogenesis of MRX because genes encoding Oligophrenin-1,[33] PAK3,[34] and ARHGEF6,[35] all of which are thought to regulate actin cytoskeleton, and are mutated in the cases of MRX. It should be noted that not all tetraspanin play a positive role in tumorigenesis or cancer metastasis. Some tetraspanins such as CD9, CD63, and CD82 are thought to function as negative regulators of metastasis.[15] In the case of CD82, a tetraspanin-associated protein, EWI-2 synergizes CD82 in inhibiting prostate cancer cell migration.[36] This discrepancy is not surprising, however, given that the function of the tetraspanin family depends on the components of tetraspanin-containing protein complex in individual cells.

TALLA-1 protein shows dot-like localization pattern in cytoplasm[37] (Figure 2C). Tetraspanin proteins are localized in various types of intracellular vesicles such as late endosomes and Weibel-Palade bodies of endothelial cells,[38,39] multivesicular major histocompatibility class II-enriched compartments of B-lymphocytes,[40] and exosomes of dendritic cells.[41,42] These data point to a possible role of tetraspanin proteins in turnover and/or sorting of tetraspanin-associated proteins. A metastatic suppressor, CD82, attenuates the epidermal growth factor (EGF) signaling by accelerating EGF receptor endocytosis via its association with the EGF receptor.[43] TALLA-1 has a tyrosine-based sorting motif at the C terminus that might recruit clathrin adapter proteins to direct the TALLA-1-containing protein complex along various trafficking routes.[44] Thus TALLA-1 may perturb normal turnover of cell surface proteins in DSRCT cells.

To elucidate the function of TALLA-1, it is necessary to characterize the TALLA-1-containing protein complex on the plasma membrane and intracellular compartments. Using recent proteomics technology, tetraspanin-associated proteins have been isolated.[36,45,46] Our preliminary analysis shows that a number of cell surface proteins are associated with TALLA-1 in Jurkat (T-ALL), IMR32 (neuroblastoma), and JN-DSRCT-1 cells. Characterization of these proteins may help in understanding the functions of TALLA-1 in tumor cells.

Acknowledgments

We thank S. Kobayashi for secretarial assistance and A. Aono, N. Hoshina, and T. Kimura for technical assistance.

References

1. Ordóñez NG: Desmoplastic small round cell tumor: I: a histopathologic study of 39 cases with emphasis on unusual histological patterns. Am J Surg Pathol 1998. 22:1303–1313
2. Ordóñez NG: Desmoplastic small round cell tumor: I: an ultrastructural and immunohistochemical study with emphasis on new immunohistochemical markers. Am J Surg Pathol 1998. 22:1314–1327
3. Gerald WL, Ladanyi M, de Alava E, Cuatrecasas M, Kushner BH, LaQuaglia MP, Rosai J: Clinical, pathologic, and molecular spectrum

of tumors associated with t(11;22)(p13;q12): desmoplastic small round-cell tumor and its variants. J Clin Oncol 1998, 16:3028–3036
4. Kim J, Pelletier J: Molecular genetics of chromosome translocations involving EWS and related family members. Physiol Genomics 1999, 1:127–138
5. Gerald WL, Rosai J, Ladanyi M: Characterization of the genomic breakpoint and chimeric transcripts in the EWS-WT1 gene fusion of desmoplastic small round cell tumor. Proc Natl Acad Sci USA 1995, 92:1028–1032
6. Kim J, Lee K, Pelletier J: The desmoplastic small round cell tumor t(11;22) translocation produces EWS/WT1 isoforms with differing oncogenic properties. Oncogene 1998, 16:1973–1979
7. Lee SB, Kolquist KA, Nichols K, Englert C, Maheswaran S, Ladanyi M, Gerald WL, Haber DA: The EWS-WT1 translocation product induces PDGFA in desmoplastic small round-cell tumour. Nat Genet 1997, 17:309–313
8. Karnieli E, Werner H, Rauscher FJ 3rd, Benjamin LE, LeRoith D: The IGF-I receptor gene promoter is a molecular target for the Ewing's sarcoma-Wilms' tumor 1 fusion protein. J Biol Chem 1996, 271: 19304–19309
9. Finkeltov I, Kuhn S, Glaser T, Idelman G, Wright JJ, Roberts CT Jr, Werner H: Transcriptional regulation of IGF-I receptor gene expression by novel isoforms of the EWS-WT1 fusion protein. Oncogene 2002, 21:1890–1898
10. Wong JC, Lee SB, Bell MD, Reynolds PA, Fiore E, Stamenkovic I, Truong V, Oliner JD, Gerald WL, Haber DA: Induction of the interleukin-2/15 receptor β-chain by the EWS-WT1 translocation product. Oncogene 2002, 21:2009–2019
11. Palmer RE, Lee SB, Wong JC, Reynolds PA, Zhang H, Truong V, Oliner JD, Gerald WL, Haber DA: Induction of BAIAP3 by the EWS-WT1 chimeric fusion implicates regulated exocytosis in tumorigenesis. Cancer Cell 2002, 2:497–505
12. Emi N, Kitaori K, Seto M, Ueda R, Saito H, Takahashi T: Isolation of a novel cDNA clone showing marked similarity to ME491/CD63 superfamily. Immunogenetics 1993, 37:193–198
13. Li SH, McInnis MG, Margolis RL, Antonarakis SE, Ross CA: Novel triplet repeat containing genes in human brain: cloning, expression, and length polymorphisms. Genomics 1993, 16:572–579
14. Stipp CS, Kolesnikova TV, Hemler ME: Functional domains in tetraspanin proteins. Trends Biochem Sci 2003, 28:106–112
15. Boucheix C, Rubinstein E: Tetraspanins. Cell Mol Life Sci 58:1189–1205, 2001
16. Nishio J, Iwasaki H, Ishiguro M, Ohjimi Y, Fujita C, Yanai F, Nibu K, Mitsudome A, Kaneko Y, Kikuchi M: Establishment and characterization of a novel human desmoplastic small round cell tumor cell line, JN-DSRCT-1. Lab Invest 2002, 82:1175–1182
17. Takagi S, Fujikawa K, Imai T, Fukuhara N, Fukudome K, Minegishi M, Tsuchiya S, Konno T, Hinuma Y, Yoshie O: Identification of a highly specific surface marker of T-cell acute lymphoblastic leukemia and neuroblastoma as a new member of the transmembrane 4 superfamily. Int J Cancer 1995, 61:706–715
18. Nakagama H, Heinrich G, Pelletier J, Housman DE: Sequence and structural requirements for high-affinity DNA binding by the WT1 gene product. Mol Cell Biol 1995, 15:1489–1498
19. Drummond IA, Rupprecht HD, Rohwer-Nutter P, Lopez-Guisa JM, Madden SL, Rauscher FJ 3rd, Sukhatme VP: DNA recognition by splicing variants of the Wilms' tumor suppressor, WT1. Mol Cell Biol 1994, 14:3800–3809
20. Kim J, Lee K, Pelletier J: The DNA binding domains of the WT1 tumor suppressor gene product and chimeric EWS/WT1 oncoprotein are functionally distinct. Oncogene 1998, 16:1021–1030
21. Hosokawa Y, Ueyama E, Morikawa Y, Maeda Y, Seto M, Senba E: Molecular cloning of a cDNA encoding mouse A15, a member of the transmembrane 4 superfamily, and its preferential expression in brain neurons. Neurosci Res 1999, 35:281–290
22. Zemni R, Bienvenu T, Vinet MC, Sefiani A, Carrie A, Billuart P, McDonell N, Couvert P, Francis F, Chafey P, Fauchereau F, Friocourt G, Portes V, Cardona A, Frints S, Meindl A, Brandau O, Ronce N, Moraine C, Bokhoven H, Ropers HH, Sudbrak R, Kahn A, Fryns JP, Beldjord C, Chelly J: A new gene involved in X-linked mental retardation identified by analysis of an X;2 balanced translocation. Nat Genet 2000, 24:167–170
23. Ono Y, Fukuhara N, Yoshie O: Transcriptional activity of TAL1 in T cell acute lymphoblastic leukemia (T-ALL) requires RBTN1 or -2 and induces TALLA1, a highly specific tumor marker of T-ALL. J Biol Chem 1997, 272:4576–4581
24. Yauch RL, Hemler ME: Specific interactions among transmembrane 4 superfamily (TM4SF) proteins and phosphoinositide 4-kinase. Biochem J 2000, 351:629–637
25. Berditchevski F: Complexes of tetraspanins with integrins: more than meets the eye. J Cell Sci 2001, 114:4143–4151
26. Yauch RL, Berditchevski F, Harler MB, Reichner J, Hemler ME: Highly stoichiometric, stable, and specific association of integrin $\alpha3\beta1$ with CD151 provides a major link to phosphatidylinositol 4-kinase, and may regulate cell migration. Mol Biol Cell 1998, 9:2751–2765
27. Yáñez-Mó M, Alfranca A, Cabañas C, Marazuela M, Tejedor R, Ursa MA, Ashman LK, de Landázuri MO, Sánchez-Madrid F: Regulation of endothelial cell motility by complexes of tetraspan molecules CD81/TAPA-1 and CD151/PETA-3 with $\alpha3\beta1$ integrin localized at endothelial lateral junctions. J Cell Biol 1998, 141:791–804
28. Zhang XA, Kazarov AR, Yang X, Bontrager AL, Stipp CS, Hemler ME: Function of the tetraspanin CD151-$\alpha6\beta1$ integrin complex during cellular morphogenesis. Mol Biol Cell 2002, 13:1–11
29. Sugiura T, Berditchevski F: Function of $\alpha3\beta1$-tetraspanin protein complexes in tumor cell invasion. Evidence for the role of the complexes in production of matrix metalloproteinase 2 (MMP-2). J Cell Biol 1999, 146:1375–1389
30. Lammerding J, Kazarov AR, Huang H, Lee RT, Hemler ME: Tetraspanin CD151 regulates $\alpha6\beta1$ integrin adhesion strengthening. Proc Natl Acad Sci USA 2003, 100:7616–7621
31. Testa JE, Brooks PC, Lin JM, Quigley JP: Eukaryotic expression cloning with an antimetastatic monoclonal antibody identifies a tetraspanin (PETA-3/CD151) as an effector of human tumor cell migration and metastasis. Cancer Res 1999, 59:3812–3820
32. Claas C, Seiter S, Claas A, Savelyeva L, Schwab M, Zoller M: Association between the rat homologue of CO-029, a metastasis-associated tetraspanin molecule and consumption coagulopathy. J Cell Biol 1998, 141:267–280
33. Billuart P, Bienvenu T, Ronce N, des Portes V, Vinet MC, Zemni R, Roest Crollius H, Carrie A, Fauchereau F, Cherry M, Briault S, Hamel B, Fryns JP, Beldjord C, Kahn A, Moraine C, Chelly J: Oligophrenin-1 encodes a rhoGAP protein involved in X-linked mental retardation. Nature 1998, 392:923–926
34. Allen KM, Gleeson JG, Bagrodia S, Partington MW, MacMillan JC, Cerione RA, Mulley JC, Walsh CA: PAK3 mutation in nonsyndromic X-linked mental retardation. Nat Genet 1998, 20:25–30
35. Kutsche K, Yntema H, Brandt A, Jantke I, Nothwang HG, Orth U, Boavida MG, David D, Chelly J, Fryns JP, Moraine C, Ropers HH, Hamel BC, van Bokhoven H, Gal A: Mutations in ARHGEF6, encoding a guanine nucleotide exchange factor for Rho GTPases, in patients with X-linked mental retardation. Nat Genet 2000, 26:247–250
36. Zhang XA, Lane WS, Charrin S, Rubinstein E, Liu L: EWI2/PGRL associates with the metastasis suppressor KAI1/CD82 and inhibits the migration of prostate cancer cells. Cancer Res 2003, 63:2665–2674
37. Azorsa DO, Moog S, Cazenave JP, Lanza F: A general approach to the generation of monoclonal antibodies against members of the tetraspanin superfamily using recombinant GST fusion proteins. J Immunol Methods 1999, 229:35–48
38. Kobayashi T, Vischer UM, Rosnoblet C, Lebrand C, Lindsay M, Parton RG, Kruithof EK, Gruenberg J: The tetraspanin CD63/lamp3 cycles between endocytic and secretory compartments in human endothelial cells. Mol Biol Cell 2000, 11:1829–1843
39. Sincock PM, Fitter S, Parton RG, Berndt MC, Gamble JR, Ashman LK: PETA-3/CD151, a member of the transmembrane 4 superfamily, is localised to the plasma membrane and endocytic system of endothelial cells, associates with multiple integrins and modulates cell function. J Cell Sci 1999, 112:833–844
40. Escola JM, Kleijmeer MJ, Stoorvogel W, Griffith JM, Yoshie O, Geuze HJ: Selective enrichment of tetraspan proteins on the internal vesicles of multivesicular endosomes and on exosomes secreted by human B-lymphocytes. J Biol Chem 1998, 273:20121–20127
41. Lamparski HG, Metha-Damani A, Yao JY, Patel S, Hsu DH, Ruegg C, Le Pecq JB: Production and characterization of clinical grade exo-

somes derived from dendritic cells. J Immunol Methods 2002, 270: 211–226
42. Zitvogel L, Regnault A, Lozier A, Wolfers J, Flament C, Tenza D, Ricciardi-Castagnoli P, Raposo G, Amigorena S: Eradication of established murine tumors using a novel cell-free vaccine: dendritic cell-derived exosomes. Nat Med 1998, 4:594–600
43. Odintsova E, Sugiura T, Berditchevski F: Attenuation of EGF receptor signaling by a metastasis suppressor, the tetraspanin CD82/KAI-1. Curr Biol 2000, 10:1009–1012
44. Bonifacino JS, Traub LM: Signals for sorting of transmembrane proteins to endosomes and lysosomes. Annu Rev Biochem 2003, 72: 395–447
45. Stipp CS, Kolesnikova TV, Hemler ME: EWI-2 is a major CD9 and CD81 partner and member of a novel Ig protein subfamily. J Biol Chem 2001, 276:40545–40554
46. Stipp CS, Orlicky D, Hemler ME: FPRP, a major, highly stoichiometric, highly specific CD81- and CD9-associated protein. J Biol Chem 2001, 276:4853–4862

Pathogenicity of autoantibodies reactive with the endogenous retroviral envelope glycoprotein gp70

M. Miyazawa[1], E. Kajiwara[1], N. Tabata[1,2], T. Ogawa[1,3], T. Yuasa[1], H. Matsumura[1]

[1]Departments of Immunology, [2]Pediatrics, and [3]Cardiovascular Surgery, Kinki University School of Medicine, Osaka-Sayama, Osaka, Japan

masaaki@med.kindai.ac.jp

Abstract

MRL/MpJ-lpr/lpr (MRL/lpr) mice spontaneously develop immune complex-mediated glomerulonephritis, granulomatous arteritis, chronic destructive arthritis, and thrombocytopenia. Recent genetic analyses in a variety of lupus-prone strains of mice have pointed out a close correlation between autoantibodies reactive with the endogenous retroviral env gene product, gp70, and the development and severity of glomerulonephritis. However, the suggested pathogenicity of anti-gp70 autoantibodies had not been directly demonstrated. To examine if anti-retroviral gp70 autoantibodies induce glomerular and vascular pathology, we established from unmanipulated MRL/lpr mice hybridoma clones that secrete monoclonal antibodies reactive with the endogenous xenotropic viral env gene product. This gp70 is known to be expressed in the liver and secreted as a normal constituent of mouse serum. A high proportion of these anti-gp70 antibody-producing hybridoma clones induced proliferative or wire loop-like glomerular lesions with massive depositions of gp70, IgG, and C3 in affected glomeruli when transplanted into syngeneic non-autoimmune or severe combined immunodeficiency mice. Furthermore, we have successfully demonstrated that repeated intravenous injections of purified monoclonal anti-gp70 autoantibodies induce glomerular pathology associated with gp70 deposition. The development of the glomerular pathology after injection of purified anti-gp70 autoantibodies was dependent on the amounts of serum gp70 expressed in the injected mice, and the development of granulomatous arteritis was also observed after repeated injections of one of the pathogenic clones of anti-gp70 autoantibodies. These results directly prove the long-debated pathogenicity of anti-retroviral autoantibodies in the mouse lupus models.

By the late 1970s a mistaken consensus emerged that viruses did not cause human cancer and that human retroviruses did not exist.

Robert C. Gallo [1]

Introduction

Nearly half century has passed since the first description of DNA-binding antibodies in the sera of patients with systemic lupus erythematosus (SLE), yet correlation between levels of anti-DNA autoantibodies and disease activity in SLE still remains controversial [2,3]. In recent cross-sectional studies, a correlation between the presence of histologically proven lupus nephritis and levels of autoantibodies reactive to double-stranded (ds) DNA has been observed [2,4]. However, most anti-DNA antibodies are actually anti-nucleosome antibodies, binding to DNA only if it is complexed to nucleosomes [3,5]. The observed nephritogenicity of experimentally established and patient-derived anti-dsDNA antibodies seems to depend on the binding of nucleosomes to the major component of glomerular basement membrane, heparan sulfate.

Pathogenicity of anti-DNA autoantibodies has been experimentally analyzed in details by using monoclonal antibodies established from mouse strains that spontaneously develop an SLE-like syndrome. These include New Zealand, MRL, and BXSB strains and their crosses, and they have provided useful tools for the immunologic and genetic dissection of pathogenetic and predisposing factors that contribute to the development of lupus-like lesions. In particular, the immunologic factors that have long been associated with the development of fatal glomerulonephritis in the above lupus-prone mice are immune complexes, anti-DNA antibodies, and antibodies reactive with the env gene product of an endogenous retrovirus, gp70 [6,7].

It has long been postulated that endogenous retroviruses might be involved in the development of human autoimmune diseases [8-10]. They may encode a part of target molecules bound by autoantibodies, or may derange and modulate immune responses through the production of superantigens, modification of cytokine gene expression, and stimulation of anti-idiotypic antibody responses. Infections with exogenous human retroviruses, HTLV-I and HIV-1, as well as exogenous retroviruses of some other species, have been associated with the development of chronic inflammatory diseases involving the central nervous system, joints, lungs, salivary glands, and blood vessels (reviewed in [9]). However, the possible involvement of endogenous retroviruses in the development of human autoimmune diseases is still controversial and largely unproven [11,12]. In contrast, there is compelling evidence indicating the involvement of endogenous retroviruses in the development of glomerulonephritis and chronic vasculitis in mouse models of systemic autoimmune diseases [8,9,13,14]. The involvement of the envelope glycoprotein gp70 of an endogenous retrovirus in the formation of circulating immune complexes, and their deposition in the glomerular and vascular lesions have been